Department of Applied Physics

Atomic-scale defects in solar cell material $CuInSe_2$ from hybrid-functional calculations

Laura Oikkonen

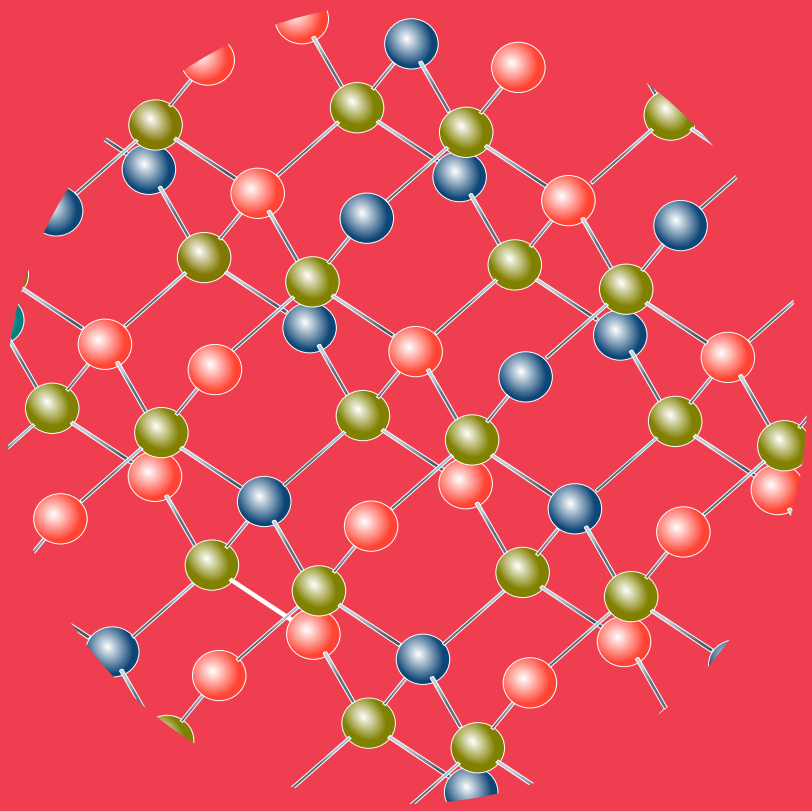

Aalto University

DOCTORAL DISSERTATIONS

Aalto University publication series
DOCTORAL DISSERTATIONS 143/2013

Atomic-scale defects in solar cell material $CuInSe_2$ from hybrid-functional calculations

Laura Oikkonen

A doctoral dissertation completed for the degree of Doctor of Science in Technology to be defended, with the permission of the Aalto University School of Science, at a public examination held at the lecture hall C of the main building on 9 October 2013 at 12.

Aalto University
School of Science
Department of Applied Physics
Electronic Properties of Materials

Supervising professor
Prof. Risto Nieminen

Thesis advisors
Dr. Maria Ganchenkova
Dr. Ari Seitsonen

Preliminary examiners
Prof. Peter Deák
University of Bremen, Germany

Dr. Hannu-Pekka Komsa
University of Helsinki, Finland

Opponents
Prof. Clas Persson
University of Oslo, Norway

Aalto University publication series
DOCTORAL DISSERTATIONS 143/2013

ISBN 978-952-60-5330-1 (printed)
ISBN 978-952-60-5331-8 (pdf)
ISSN-L 1799-4934
ISSN 1799-4934 (printed)
ISSN 1799-4942 (pdf)
http://urn.fi/URN:ISBN:978-952-60-5331-8

Unigrafia Oy
Helsinki 2013

Finland

Publication orders (printed book):
laura.oikkonen@aalto.fi

Aalto University

Abstract

Aalto University, P.O. Box 11000, FI-00076 Aalto www.aalto.fi

Author
Laura Oikkonen

Name of the doctoral dissertation
Atomic-scale defects in solar cell material $CuInSe_2$ from hybrid-functional calculations

Publisher School of Science

Unit Department of Applied Physics

Series Aalto University publication series DOCTORAL DISSERTATIONS 143/2013

Field of research Theoretical and computational physics

Manuscript submitted 10 June 2013 **Date of the defence** 9 October 2013

Permission to publish granted (date) 16 August 2013 **Language** English

☐ **Monograph** ☒ **Article dissertation (summary + original articles)**

Abstract

The operation and properties of any semiconductor device rely on its defect microstructure. In thin-film solar cells, point defects are a determining factor for the conversion efficiency of the device by controlling doping but also by degrading device performance. Additionally, point defects play a role in material growth and processing by mediating diffusion. Knowledge of point defects and defect-related processes is therefore essential in optimizing solar cell performance.

In this thesis, point defects in the solar cell absorber material $CuInSe_2$ (CIS) have been investigated with computational methods. Starting from the thermodynamics of individual point defects and extending to diffusion kinetics and clustering, the aim of the thesis is to gain a comprehensive understanding of the defect microstructural features of the material and their effect on its electronic properties. The calculations have been performed with density-functional theory (DFT) employing a hybrid exchange-correlation functional, which has been demonstrated to describe semiconductor properties better than previously used (semi)local-density functionals.

The calculations presented in this thesis show that point defects in CIS participate in a variety of competing atomic-scale processes, which affect their distribution within the material. By taking into account defect interactions, it is demonstrated that there exists a thermodynamic driving force towards the creation of defect complexes such as In_{Cu}-$2V_{Cu}$ and V_{Se}-V_{Cu}. Interaction of intrinsic defects with impurities can also lead to surprising effects: it is found that by introducing sodium atoms into CIS, copper mass transport is reduced due to the capture of copper vacancies. The effect of the prevalent point defects and defect complexes on the electronic properties is found to essentially depend on whether the defect is of cationic or anionic type. Only selenium-related anionic defects are observed to induce deep defect levels within the CIS band gap, implying that they may act as recombination centers.

The results presented in this thesis help to explain and interpret experimental observations of atomic-scale phenomena occurring in CIS. Further, they provide computational insight on defect-related mechanisms that may sometimes remain out of reach in experiments. The findings can be employed to gain better control over film quality and device operation in CIS-based solar cells.

Keywords point defects, density-functional theory, electronic structure calculations, atomic diffusion

ISBN (printed) 978-952-60-5330-1 **ISBN (pdf)** 978-952-60-5331-8

ISSN-L 1799-4934 **ISSN (printed)** 1799-4934 **ISSN (pdf)** 1799-4942

Location of publisher Helsinki **Location of printing** Helsinki **Year** 2013

Pages 103 **urn** http://urn.fi/URN:ISBN:978-952-60-5331-8

A? Aalto-yliopisto

Tiivistelmä

Aalto-yliopisto, PL 11000, 00076 Aalto www.aalto.fi

Tekijä
Laura Oikkonen

Väitöskirjan nimi
Pistemäisten hilavirheiden mallintaminen $CuInSe_2$ -aurinkokennomateriaalissa

Julkaisija Perustieteiden korkeakoulu

Yksikkö Teknillisen fysiikan laitos

Sarja Aalto University publication series DOCTORAL DISSERTATIONS 143/2013

Tutkimusala Teoreettinen ja laskennallinen fysiikka

Käsikirjoituksen pvm 10.06.2013 **Väitöspäivä** 09.10.2013

Julkaisuluvan myöntämispäivä 16.08.2013 **Kieli** Englanti

☐ **Monografia** ☒ **Yhdistelmäväitöskirja (yhteenveto-osa + erillisartikkelit)**

Tiivistelmä

Puolijohdeteknologia perustuu suurilta osin pistemäisten hilavirheiden hallittuun käyttöön. Esimerkiksi ohutkalvoaurinkokennoissa pistemäiset hilavirheet määrittävät laitteen hyötysuhdetta: ne luovuttavat varauksenkuljettajia, mutta saattavat myös haitata laitteen toimintaa. Lisäksi ne vaikuttavat materiaalin kasvatuksen ja käsittelyn aikana toimimalla diffuusion välittäjinä. Aurinkokennojen hyötysuhteen parantamiseksi onkin siis tärkeää tuntea hilavirheet ja niihin liittyvät mekanismit.

Tässä väitöskirjassa on tutkittu pistemäisiä hilavirheitä $CuInSe_2$-aurinkokennomateriaalissa (CIS) laskennallisen mallinnuksen avulla. Väitöskirjan tavoitteena on hahmottaa kokonaisvaltaisesti materiaalin atomitason rakennetta sekä sen vaikutusta sähköisiin ominaisuuksiin. Tutkimus ulottuu yksittäisistä pistemäisistä hilavirheistä aina hilavirheiden keskinäisiin vuorovaikutuksiin asti. Mallinnus pohjautuu tiheysfunktionaaliteoriaan, ja vaihto−korrelaatio -vuorovaikutusta on kuvattu ns. hybridifunktionaalilla. Hybridifunktionaalien on osoitettu kuvaavan puolijohdemateriaalien ominaisuuksia paremmin kuin aiemmin käytettyjen, pelkästään paikalliseen tiheyteen perustuvien approksimaatioiden.

Väitöskirjan tulokset osoittavat, että monenlaiset atomimittaluokan prosessit vaikuttavat pistemäisten hilavirheiden levittäytymiseen kidehilassa. Keskinäisten vuorovaikutusten tuloksena hilavirheet voivat ajautua muodostamaan ryppäitä kuten In_{Cu}-$2V_{Cu}$ ja V_{Se}-V_{Cu}. Hilavirheiden ja epäpuhtausatomien väliset vuorovaikutukset voivat myös aiheuttaa yllättäviä ilmiöitä: natriumatomien lisäämisen huomattiin vähentävän kuparin diffuusiota CIS:ssä kuparivakanssien loukkuuntumisen takia. Yleisimpien pistemäisten hilavirheiden huomattiin vaikuttavan aineen sähköisiin ominaisuuksiin eri tavoin niiden tyypistä riippuen: ainoastaan seleenityyppisten hilavirheiden havaittiin synnyttävän syviä epäpuhtaustiloja CIS:n energia-aukkoon, joten ne saattavat toimia rekombinaatiokeskuksina.

Tässä väitöskirjassa esitettyjen tulosten avulla voidaan tulkita ja selittää kokeellisia havaintoja CIS:ssä tapahtuvista atomitason ilmiöistä. Lisäksi tulokset auttavat ymmärtämään hilavirheisiin liittyviä mekanismeja, joista osa on toistaiseksi kokeellisten menetelmien ulottumattomissa. Tuloksia voidaan käyttää ohutkalvojen laadun sekä CIS-pohjaisten aurinkokennojen toiminnan hallittuun parantamiseen.

Avainsanat hilavirheet, tiheysfunktionaaliteoria, elektronirakennelaskut, diffuusio

ISBN (painettu) 978-952-60-5330-1 **ISBN (pdf)** 978-952-60-5331-8

ISSN-L 1799-4934 **ISSN (painettu)** 1799-4934 **ISSN (pdf)** 1799-4942

Julkaisupaikka Helsinki **Painopaikka** Helsinki **Vuosi** 2013

Sivumäärä 103 **urn** http://urn.fi/URN:ISBN:978-952-60-5331-8

Preface

The work presented in this thesis has been carried out at the Center of Excellence in Computational Nanoscience (COMP) at the Department of Applied Physics, Aalto University, during the years 2008-2013. I wish to express my gratitude to my supervisor, Prof. Risto Nieminen, for giving me this opportunity to learn and build my path in science, as well as for his guidance during these years. I would also like to thank the leader of the Electronic Properties of Materials group, Prof. Martti Puska, for providing such a great international research community within our group.

I am indebted to Dr. Maria Ganchenkova, whose guidance, support, and cheerfulness have helped and inspired me constantly during the course of this thesis work. Dr. Ari Seitsonen from University of Zürich kindly provided us with his expertise and attention to detail, which was greatly appreciated. Be it the practicalities of running a simulation or visualizing the results, I have always been able to rely on the skills and patience of Dr. Timo Vehviläinen. The computational work in this thesis would not have been possible without the generous allocation of resources from the Finnish Center for Scientific Computing (CSC) as well as from our Department of Applied Physics.

I also wish to express my gratitude to all the other wonderful people, both in and outside the Department, who I have met during the course of my PhD studies and who have inspired me along the way. Final thanks go to my friends and family, especially my parents for encouragement; my sister, Salla, for recognizing the importance of celebration; and my husband, Sakari, for tea and sympathy.

Helsinki, September 11, 2013,

Laura Oikkonen

Contents

Preface i

Contents iii

List of Publications v

Author's Contribution vii

1. Introduction 1

1.1 Background and research environment: The importance of point defects in materials research and applications 1

1.2 Objectives and scope: Point defects in $CuInSe_2$ 2

2. Literature review 7

3. Methods 11

3.1 Basics of density-functional theory 11

3.2 Modeling the exchange-correlation energy 12

3.3 Implementation of density-functional theory in practice . . . 14

3.4 Point defect calculations 16

3.4.1 Finite-size corrections 17

3.4.2 Accuracy of calculations 19

4. Results 21

4.1 Formation energies: Which point defects exist in CIS? 21

4.2 Diffusion kinetics: How do point defects migrate in CIS? . . 24

4.3 Defect interactions: Which kinds of complexes can point defects form in CIS? 27

4.4 Band structures: How do point defects modify the electronic properties of CIS? 29

5. Discussion and outlook **33**

5.1 Critical evaluation of exchange-correlation functionals . . . 33

5.2 Practical implications 36

Bibliography **39**

Publications **45**

List of Publications

This thesis consists of an overview and of the following publications which are referred to in the text by their Roman numerals.

I Oikkonen, L.E., Ganchenkova, M.G., Seitsonen, A.P., and Nieminen, R.M. Vacancies in $CuInSe_2$: new insights from hybrid-functional calculations. *Journal of Physics: Condensed Matter*, 23, 422202, October 2011.

II Oikkonen, L.E., Ganchenkova, M.G., Seitsonen, A.P., and Nieminen, R.M. Redirecting focus in $CuInSe_2$ defect studies towards selenium-related defects. *Physical Review B*, 86, 165115, October 2012.

III Oikkonen, L.E., Ganchenkova, M.G., Seitsonen, A.P., and Nieminen, R.M. Mass transport in $CuInSe_2$ from first principles. *Journal of Applied Physics*, 113, 133510, April 2013.

IV Oikkonen, L.E., Ganchenkova, M.G., Seitsonen, A.P., and Nieminen, R.M. Formation, migration, and clustering of point defects in $CuInSe_2$ from first principles. Submitted to *Physical Review B*, May 2013.

V Oikkonen, L.E., Ganchenkova, M.G., Seitsonen, A.P., and Nieminen, R.M. Effect of sodium incorporation into $CuInSe_2$ from first principles. *Journal of Applied Physics*, 114, 083503, August 2013.

Author's Contribution

The author is the main contributor for Publications I-V and has had an active role in all the phases of the research reported in this thesis. She has carried out all the presented first-principles calculations and written the main drafts of all the publications.

1. Introduction

1.1 Background and research environment: The importance of point defects in materials research and applications

No crystalline material is perfect from the structural point of view. The periodic arrays of atoms constituting solids are constantly disrupted by atomic-scale imperfections of various kinds, collectively referred to as point defects. Some of these imperfections – missing atoms called vacancies, misplaced atoms called antisites, or additional atoms called interstitials – arise from configurational entropy and exist inherently in crystals. Other kinds of point defects involving foreign atoms may be incorporated, either intentionally or unintentionally, into crystals during growth and processing. Together, they dictate to a great extent the electronic and optical properties of a material [1].

The role of point defects in determining material properties is widely recognized and exploited in technological applications. In particular, point defects acting in semiconductors form the basis for the entire electronics industry, enabling the functioning of devices such as microcircuits, diodes, optoelectronics, and solar cells. The conductivity of an electronic device is typically tuned by the controlled addition of foreign atoms in a process called doping. At the same time, conductivity is affected by native or unintentionally incorporated point defects, which may deteriorate the operation of the device by charge compensation, the creation of recombination centers, or by pinning the Fermi level. Apart from this, the effect of native defects also pertains to kinetics during growth, processing, and operation since they mediate diffusion and thus direct the microkinetic formation of the material.

The successful fabrication and reliable operation of a semiconductor de-

vice requires detailed knowledge of its defects: both the beneficial and detrimental effects they may cause in the material. This has made research on point defects a very active field of materials physics. Diverse experimental approaches are employed for defect characterization to probe various defect-related properties such as lattice relaxations, ionization levels, and defect concentrations. Yet, in practice, these methods are often limited in their application (see e.g. Ref. [2] and references therein) with respect to sample quality and experimental conditions. Further, their use typically requires a high degree of sophistication in order to exclude contributions from other defects. Even when proper conditions are met, central defect-related quantities such as defect concentrations or migration barriers cannot be directly measured but must rather be deduced from other observations. As a result, information extracted from experiments remains very sensitive to interpretation.

Faced with the experimental challenges for defect characterization, computational methods have become increasingly important in complementing experiments in the identification of point defects. Density-functional theory (DFT), in particular, has been widely successful not only in reproducing but also in predicting material properties from first principles [3]. Theoretical simulations allow studying a chosen physical system in an idealized setup including, for instance, one point defect at a time in the absence any unwanted disturbances. Consequently, DFT calculations can provide a link between an experimentally detected property and the causing structural item. Moreover, interactions between defects may also be investigated to gain insight on defect-mediated diffusion mechanisms and microstructure formation in materials, shedding light on aspects of defect physics that may sometimes remain out of reach in experiments. The capabilities of theoretical methods continue to grow with the advances in computational capacity.

1.2 Objectives and scope: Point defects in $CuInSe_2$

In this thesis, point defects have been studied with density-functional theory in the solar cell absorber material $CuInSe_2$ (CIS). Solar cells incorporating CIS and its alloy $Cu(In,Ga)Se_2$ (CIGS), where In has been partly replaced by Ga, represent the most successful thin-film solar cell technology in terms of both laboratory scale and commercial use. The record conversion efficiency for CIGS cells has been steadily increasing for the past

30 years and recently surpassed 20% [4]. Yet even greater efficiencies are required to truly challenge the dominance of wafer-based silicon technology in the solar energy business. The development of silicon solar cells has benefited from an extensive knowledge base accumulated within the microelectronics industry, compared to which the degree of understanding of the role of defects in CIS remains very limited. In fact, the lack of knowledge has hindered the systematic development of CIGS technology, which has had to mostly rely on empirical trial and error instead of well-targeted defect engineering [5, 6].

The uncertainties related to defect physics in CIS pertain to defect properties and mechanisms of defect-mediated processes, which are as crucial in solar cells as in any semiconductor device. Extensive experimental efforts have unfortunately not brought full clarity on these issues – as described in Section 1.1, relating particular point defects to experimentally observed phenomena is often very sensitive to interpretation. Interpretations become even more ambiguous in a ternary material such as CIS, where contributions can arise from twelve different kinds of native point defects, not to mention the possible defect complexes or unwanted impurities. For instance, while experimental methods such as photoluminescence, cathodoluminescence, and time-dependent Hall measurements, probing the electronic structure of chalcopyrite materials, suggest the presence of four shallow [7, 8, 9] and two deep defect levels [10, 11] within the band gap, these levels have not been correlated with any structural defect. In some cases, it is not even clear whether a given level originates from bulk, interface regions, or some completely separate phenomenon [12, 13]. Moreover, positron-annihilation-spectroscopy (PAS) studies [14, 15, 16, 17] exploring vacancy-type defects have observed monovacancies and small vacancy clusters in CIS-based thin films, whose identities cannot be further specified. With respect to defect kinetics, self-diffusion data recorded in chalcopyrite thin-film samples is so scarce and shows such a wide scatter that it does not allow drawing conclusions on the operating diffusion mechanisms (see e.g. Refs. [18, 19] and references therein).

From the computational side, point defects in CIS have also been studied [19, 20, 21, 22, 23, 24, 25, 26, 27, 28, 29, 30, 31, 32] but not to such an extent as in many other technologically relevant semiconductors. The majority of these studies has been conducted within the local-density approximation (LDA) implementation of DFT, which suffers from an underesti-

mation of semiconductor band gaps of typically 50%. The underestimation is especially pronounced in materials with strongly localized d states such as CIS, for which LDA incorrectly gives a metallic ground state. The vanishing band gap together with computational restrictions on the supercell size have led to broad uncertainty ranges for various defect-related quantities such as charge transition levels. Consequently, the results concerning defect identification have practically remained at the level of speculations, and no strict correspondence between theory and experiment has been obtained [33].

Nonetheless, the scarcity of existing overlapping studies from independent research groups has led to a situation where the computational results on CIS may have been accepted slightly too easily. In the case of other semiconductors such as nitrides or zinc oxide, the role of point defects has provoked fierce debates among theorists [34, 35, 36, 37]. In contrast, regarding CIS, the difference between speculations and facts has become obscure after the relatively few computational results have been quoted and used eagerly in the subsequent interpretation of experimental observations. Though unintentional, this may also have created a self-consistency loop, where experiments have been interpreted based on theory, which in turn has been strongly experiment-driven and has been influenced by careful considerations of the intuition of experimentalists.

The starting point of this thesis is decidedly different: returning to pure theory, first-principles calculations, and leaving aside for a while everything that has been speculated to be known about point defects in CIS. This is made possible, in part, by the recent development in the implementation of DFT, namely, hybrid exchange-correlation functionals [38]. Hybrid functionals have been shown to improve the description of CIS material properties, including the band gap, compared to (semi)local approximations [19, 39, 40]. By eliminating the need for *a posteriori* gap corrections, hybrid functionals also increase transparency in the methodology.

It should be emphasized that the purpose of this work is not to keep theory separate from real materials; indeed, the power to describe and predict material properties is the main justification for the existence and development of theoretical methodology, and calculations should always be compared with experiment when comparison is appropriate and commensurate. However, it should not be a goal in itself to force seeming correspondence with experiment starting from the ingredients at hand.

For this reason, the strengths and weaknesses of the methodology used in this work are also critically assessed.

In this thesis, the role of point defects in CIS has been investigated starting from their characterization and extending to defect-related phenomena such as diffusion and clustering. The considered point defects include intrinsic defects as well as sodium, which is a technologically relevant impurity in CIS. The results of the thesis can be divided under four research questions:

- What are the most likely point defects in CIS?
  This question has been answered in Publications I, IV, and V.

- How do point defects migrate in CIS?
  This question has been answered in Publications III and IV.

- Which kinds of complexes can point defects form in CIS?
  This question has been answered in Publications IV and V.

- How do point defects modify the electronic properties of CIS?
  This question has been answered in Publications II and IV.

This thesis is organized as follows: In Chapter 2, the history of point defect calculations in CIS is outlined starting from the cavity model up to the recent progress made with hybrid exchange-correlation functionals. In Chapter 3, the methodology employed in the computational modeling of point defects is presented, including a brief overview of DFT and the most important questions concerning the choices in parameters and functionals. In Chapter 4, each research question is answered concisely. In Chapter 5, the results are compared with previously reported ones, and their accuracy is critically assessed. Further, the results and their impact are discussed from the practical point of view.

2. Literature review

The progress in modeling point defects in CIS has followed the evolution of computational methods, which in turn is closely linked with the capabilities provided by computational power. Throughout, calculations have been motivated by a strong desire to understand the defect physics of the material as well as to support the experimental development of thin-film solar cells. Computational methods face limitations of their own, yet it seems that the deficiencies of each method have been fully acknowledged only after the emergence of a better approach.

One of the fundamental questions in characterizing a semiconductor material is identifying the main point defects and their contribution to the doping behavior. Following the experimental development of CIS-based solar cells that had fully started in the 1970s in Bell Labs [33], the first attempts to estimate defect formation energies were made in the 1980s employing a generalization of the cavity model of Van Vechten [23]. The cavity model used empirical atomic radii and model bond lengths as input to simulate atomic properties. Selected point defects were placed in order of increasing formation energies (see Figure 2.1), with the antisites $\mathrm{In_{Cu}}$ and $\mathrm{Cu_{In}}$ being energetically most favorable, followed by the three vacancies V_{Se}, V_{Cu} and V_{In}, respectively, and the copper interstitial as the least favorable point defect. These findings were subsequently used to interpret characterization experiments, assuming $\mathrm{In_{Cu}}$ to be the dominant point defect in the material.

The results based on the cavity model were, however, eventually laid aside with the advances in *ab initio* calculations. Electronic-structure calculations based on density-functional theory did not require any other input parameters apart from specifying atomic species, thus providing an easily applicable framework for different kinds of systems. The properties of bulk CIS had already been studied with DFT methods by Jaffe and

Zunger [41, 42], who for instance explained the features arising in the band structure of chalcopyrite materials. DFT calculations within the local-density approximation (LDA) were first applied to defects in CIS by Zunger's group [24, 43], showing a marked step forward from the times of the cavity model.

Along several years, Zunger's group made several important contributions to understanding CIS defect physics, which remain to this day the most cited works in the field [24, 26, 27, 28, 30, 32]. They calculated charge transition levels and re-evaluated the formation energies previously considered within the cavity model, obtaining differing results for the energetic preference among the defects as displayed in Figure 2.1. Most notably, copper vacancy rose alongside the cationic antisites as one of the most important point defects in CIS. This was supported by experimental observations of the ease of growing copper-poor CIS material [6]. Additionally, some of the point defects were suggested to occur as complexes, which was invoked to explain the existence of tens of related crystal structures and the tolerance to off-stoichiometry [24, 43]. Further, the point defects V_{Se}, V_{Cu}-V_{Se}, and $\mathrm{In}_{\mathrm{Cu}}^{\mathrm{DX}}$ were related to experimentally observed metastable electrical behavior such as the persistent p-type conductivity and red-on-bias metastability [28, 30, 32]. In Zunger's wake, a few studies repeating their computational procedure for the most basic defects and, not surprisingly, validating their results followed [25, 29, 31].

A major drawback of LDA employed in these studies was, however, its representation of semiconductor band gaps, which were severely underestimated due to an inadequate description of electron-electron interactions. To make things worse, the supercell implementation commonly used for point defect calculations gave rise to finite-size effects, which greatly affected the total energies of the defect systems. The finite-size effects could be alleviated by increasing the supercell size, but the computations at the time were restricted to supercells of only 32 and, later, 64 atoms. These

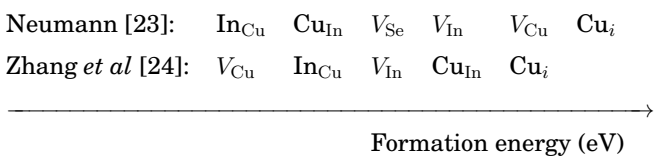

Figure 2.1. Energetic order of preference of various point defects in CIS according to Refs. [23, 24]: the higher the formation energy, the less favorable the defect is. The ordering in Ref. [24] has been derived under Cu-poor and In-rich conditions.

two issues had to be tackled in order to obtain realistic results.

In their early work, Zunger's group used the scissor scheme to open up the CIS band gap [24]. Later on, they switched to aligning the valence-band maximum (VBM) with LDA+U, a method incorporating a localized energy term to the problematic Cu 3d orbitals, followed by the scissor scheme. The finite-size errors were dealt with a combination of the potential alignment scheme and Makov-Payne corrections [44]. At the same time, these corrections brought along uncertainties whose magnitude is difficult to evaluate, and therefore the subsequent interpretations of experimentally detected ionization levels should be dealt with caution.

Only in recent years, with the advances in computational capacity, LDA has been exceeded by hybrid exchange-correlation functionals incorporating a portion of exact exchange. In the case of CIS, a hybrid functional such as HSE06 has led to a drastically improved electronic structure, including a far more realistic band gap than before as well as a better description of structural properties, giving hope of increasing accuracy also regarding defect calculations. HSE06 was soon put into use, and publications reporting updated results on defect energetics started to appear [19, 21, 22, 40]. Though HSE06 has been able to alleviate the band gap problem, the finite-size problem has remained, or even got worse: as HSE06 calculations are much more computationally intensive than LDA calculations, which have already reached the size of thousands of atoms for certain systems, HSE06 has had to settle with systems consisting of a couple of hundred atoms at most.

Meanwhile, CIS has been fervently studied experimentally without appreciable additions in understanding. It seems that the material is intrinsically so complex that the various atomic-scale processes cannot be disentangled from each other. Theoretical methods, therefore, continue to defend their place not only in supplementing experiment but also providing means for interpreting observations – as long as their deficiencies are properly taken into account.

3. Methods

3.1 Basics of density-functional theory

Modeling of an atomic system involves dealing with a multitude of interactions between the constituent particles. The challenge is to retain the essential features of the many-body interactions while still keeping the problem computationally tractable to solve. As the most widely used method for electronic-structure calculations, density-functional theory (DFT) has succeeded in not only reproducing but also predicting the properties of a large variety of materials. Instead of treating all interactions explicitly, electrons are studied as independent particles moving in an effective potential in a mean-field-like manner in the Kohn-Sham formalism of DFT. In the following, the main points of density-functional theory are summarized along with a description of its most notable failures.

The interaction between two quantum-mechanical particles can be described exactly starting from the Schrödinger equation. However, already the addition of a third particle to the system renders the problem overly complex to be solved analytically. Further, in a system consisting of N electrons, where each electron increases the dimensionality of the system by three, the system size soon increases not only beyond analytically tractable, but also numerically tractable.

The core idea behind DFT is that all observables of an atomic system can be expressed in terms of electronic density, which depends on only three coordinates, instead of wavefunctions with $3N$ degrees of freedom. For instance, the total energy of the system becomes a unique functional of the electronic density $n(\mathbf{r})$ [45]:

$$E[n] = T[n] + E_{\mathrm{ne}}[n] + E_{\mathrm{H}}[n] + E_{\mathrm{xc}}[n], \tag{3.1}$$

where T denotes the kinetic energy of the electrons, E_{ne} is the external po-

tential energy (typically arising from interactions with nuclei), E_{H} is the electrostatic interaction energy between electrons (also known as Hartree energy), and E_{xc} is the exchange-correlation energy.

The electronic density $n(\mathbf{r})$ minimizing the energy functional $E[n]$ corresponds to the ground state of the system. The only constraint imposed on n is that it must conserve the number of electrons, N, in the system:

$$\int n(\mathbf{r}) d\mathbf{r} = N. \tag{3.2}$$

It turns out that the terms appearing in Equation 3.1 are better expressed with respect to single-particle orbitals $\phi_i(\mathbf{r})$ rather than n explicitly. The only term whose analytical form is not known is E_{xc}, whose contribution to $E[n]$ is typically the smallest. The original many-electron system can thus be replaced by N single-particle Schrödinger equations called the Kohn-Sham equations [46]:

$$\left[-\frac{1}{2}\nabla^2 + \underbrace{V_{\mathrm{ext}}(\mathbf{r}) + V_{\mathrm{H}}(\mathbf{r}) + V_{\mathrm{xc}}(\mathbf{r})}_{V_{\mathrm{eff}}(\mathbf{r})} \right] \phi_i(\mathbf{r}) = \epsilon_i \phi_i(\mathbf{r}), \tag{3.3}$$

where V_{ext} is the external potential, V_{H} is the Hartree potential, and V_{xc} is the exchange-correlation potential. The effective potential, V_{eff}, must be solved self-consistently with the resulting density. It should be noted that the eigenvalues ϵ_i appearing in Equation 3.3 are not physical energies but Lagrange multipliers arising from the minimization constraint. Similarly, the orbitals ϕ_i are not electron orbitals although they are orthonormal and their overall density must reproduce the electronic density n of the system such that $n(\mathbf{r}) = \sum_i |\phi_i(\mathbf{r})|^2$. In fact, only the total energy and density obtained from the Kohn-Sham formalism are physically meaningful quantities [3]. While in principle, DFT could provide an exact description of the ground state of the system, in practice its implementation within the Kohn-Sham formalism is limited by the accuracy of the approximation used for the exchange-correlation functional.

3.2 Modeling the exchange-correlation energy

As its name implies, the exchange-correlation interaction between electrons consists of two contributions: exchange and correlation. Exchange arises from the Pauli principle according to which any two electrons cannot occupy the same quantum-mechanical state. Correlation encompasses screening effects of electrons, whereby electrons collectively correlate to

reduce the net interaction among any two electrons. Capturing these effects within some approximation in a satisfactory way has been a long-standing problem within the DFT community [3].

The simplest and most widely used approximation for the exchange-correlation energy is the local-density approximation (LDA). LDA is based on the observation that densities typically found in solids resemble that of a homogeneous electron gas, where the range of the effects of exchange and correlation is rather short. Therefore, E_{xc} can be approximated locally as the energy of a homogeneous electron gas with the same density n. LDA has been found to provide surprisingly accurate predictions of experimental results for a wide range of materials, though it shows clear preference for systems with slowly varying electron densities. Delocalizing electronic densities causes excessive bonding in atomic systems, leading to an overestimation of binding energies and underestimation of bond lengths. Systems lying completely beyond the reach of LDA are those that do not resemble non-interacting electron gases, such as strongly correlated materials [46, 47].

LDA has also been extended to include gradients of density in the so-called generalized-gradient approximation (GGA). However, GGA does not provide consistent improvement over LDA and does not succeed in overcoming the fundamental deficiencies of LDA [48].

The notable deficiencies of (semi)local approximations are essentially two: the presence of self-interaction and the lack of derivative discontinuities in the exchange-correlation energy. Self-interaction arises from the mean-field theory due to the fact that each electron interacts also with itself through the effective potential. The absence of derivative discontinuities reflects the incorrect convex behavior of the local functionals with respect to fractional level occupation [49]. These shortcomings lead, for instance, to an unphysical delocalization of localized states and an underestimation of band gaps.

The self-interaction error is avoided in another non-interacting electron method, namely, Hartree-Fock. In the Hartree-Fock approach, the many-electron wavefunction is written as an antisymmetrized product of orbitals, and the explicit inclusion of exchange between all orbitals exactly cancels their self-interaction. As a downside, correlation effects are neglected altogether, resulting in a lack of derivative discontinuities with an unphysical preference for integer occupancies. This results in opposite effects compared to (semi)local-density approximations: an overlocaliza-

tion of states and an overestimation of band gaps.

Since the deficiencies of the Kohn-Sham and Hartree-Fock approaches appear complementary, the two methods have been brought together as an attempt to improve the description of band gaps and other material properties, resulting in the creation of hybrid functionals [48, 50]. A hybrid exchange-correlation functional is usually constructed from a portion of exact exchange from Hartree-Fock and correlation from a GGA-type PBE (Perdew-Burke-Ernzerhof) functional [51, 52]:

$$E_{\mathrm{xc}}^{\mathrm{hybrid}} = \alpha E_{\mathrm{x}}^{\mathrm{HF}} + (1-\alpha) E_{\mathrm{x}}^{\mathrm{PBE\text{-}GGA}} + E_{\mathrm{c}}^{\mathrm{PBE\text{-}GGA}}, \tag{3.4}$$

where x denotes exchange and c denotes correlation. The fraction of exact exchange, α, can in principle be tuned, although its default value of 0.25 has been derived from perturbation theory [51]. Computing the Hartree-Fock part is typically one order of magnitude more expensive than PBE-GGA due to the slow decay of the exchange interaction with distance.

A further improved version of hybrid functionals takes into account the fact that electron-electron interactions are screened off at longer distances in extended systems. The non-local exchange is therefore separated into two parts − long range and short range − and only the latter is included, reducing the computational time. The exchange-correlation energy of this functional, proposed by Heyd, Scuseria, and Ernzerhof (HSE) [38, 53], is thus expressed as:

$$E_{\mathrm{xc}}^{\mathrm{HSE}} = \frac{1}{4} E_{\mathrm{x}}^{\mathrm{sr,HF}} + \frac{3}{4} E_{\mathrm{x}}^{\mathrm{sr,PBE\text{-}GGA}} + E_{\mathrm{x}}^{\mathrm{lr,PBE\text{-}GGA}} + E_{\mathrm{c}}^{\mathrm{PBE\text{-}GGA}}, \tag{3.5}$$

where sr and lr denote short range and long range, respectively. The tunable range-separation parameter, ω, determines the cutoff distance beyond which the short-range interaction becomes negligible. In the HSE06 functional, this value has been set to 0.2 1/Å. As expected, hybrid functionals have demonstrated an improved description of material properties compared to (semi)local-density approximations or Hartree-Fock.

3.3 Implementation of density-functional theory in practice

The computational routine for solving the ground state of an atomic system has been implemented in several computer codes, of which Vienna *Ab initio* Simulation Package (VASP) [56, 57] has been used in this thesis. To solve the Kohn-Sham equations, the system is transformed onto a chosen set of basis functions. Some typical choices include plane waves, gaussian orbitals, or atomic orbitals. VASP uses a plane-wave basis, which

Table 3.1. Calculated lattice constants a and c and band gap E_g of $CuInSe_2$.

	a (Å)	$c/2$ (Å)	E_g (eV)
PBE-GGA	5.871	5.909	0.01
HSE06	5.824	5.866	0.86
Exp.	5.781[54]	5.809[54]	1.04[55]

is often considered the most advantageous due to its completeness, manageability, and independence from energy or the positions of atoms [56]. However, the electronic wavefunctions can be difficult to reproduce in the plane-wave basis: the strong ionic potential in the core region results in rapid oscillations, which require a large number of plane waves [58]. The number of plane waves employed in the calculations is determined by setting a cutoff energy to their kinetic energies (400 eV in this work). The wavefunction is evaluated at specific k points in the reciprocal space.

Several approaches have been developed to model the interaction between ions and electrons. In this work, the projector-augmented-wave (PAW) method has been employed [59]. The PAW method is an exact all-electron method for a complete set of partial waves: the exact wavefunctions are reconstructed in the core region such that no information is lost on the full charge and spin densities. It also ensures orthogonality between valence and core wavefunctions.

Yet another technical choice characterizing DFT calculations is selecting an exchange-correlation functional to model electron-electron interactions (see Section 3.2). In this thesis, the calculations have been performed employing the HSE06 functional with the default parameter settings of α=0.25 and ω=0.20 1/Å. In specific cases, also the computationally less expensive PBE-GGA functional has been employed. The fundamental bulk properties of CIS obtained with these two functionals are listed in Table 3.1.

After solving iteratively the Kohn-Sham equations, the ground-state energy corresponding to the electronic density can be determined from Equation 3.1. Knowing this energy, the forces on the ions are calculated as derivatives of the free energy with respect to ionic positions following the Hellmann-Feynman theorem [60]. The ions are moved according to these forces, after which a new set of electronic wavefunctions is generated for the new structure. This cycle is repeated until the lowest-energy state is reached. The convergence criteria can be set in terms of an en-

ergy difference between two consecutive iteration steps or an upper limit for the forces on each atom.

3.4 Point defect calculations

Defect calculations are typically carried out by embedding a point defect into a finite-sized supercell. The supercell is repeated throughout space via periodic boundary conditions to create an infinite crystal as shown in Figure 3.1. This procedure allows the determination of quantities such as defect formation energies E_f and charge transition levels $\epsilon(q/q')$. Meanwhile, the finite size of the supercell gives rise to spurious effects, which should be carefully corrected in order to obtain physically meaningful results. In the following, the calculation procedures for various defect-related quantities are described along with correction methods that can be used to address the finite-size errors.

A point defect is created in a perfect crystal by adding and/or removing n_i atoms of type i from the bulk supercell. The formation energy of each defect is calculated as:

$$E_f^q = E_{\text{defect}}^q - E_{\text{bulk}} \pm \sum_i n_i \mu_i + q(E_{\text{VBM}} + \mu_e). \tag{3.6}$$

E_{bulk} denotes the total energy of the bulk supercell and E_{defect}^q is the total energy of the supercell containing the defect in charge state q. The chemical potential, μ_i, indicates how much energy is needed to exchange an

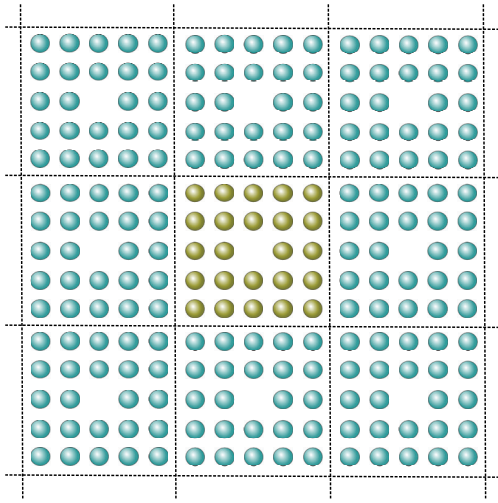

Figure 3.1. Schematic illustration of the supercell approach. A supercell containing a vacancy is repeated in all directions via periodic boundary conditions.

atom of type i between a homogeneous particle reservoir and the system. The Fermi level position, also known as the electron chemical potential, μ_e, is referenced to the energy at the valence band maximum, E_{VBM}, and is allowed to vary between 0 and E_g (for more details, see e.g. Ref. [61]).

The chemical potentials μ_i can be expressed with respect to the chemical potentials of elemental solids μ_i^0: $\mu_i = \mu_i^0 + \Delta\mu_i$. In the case of CIS, the elemental chemical potentials have been evaluated for fcc Cu, bct In, and trigonal Se. $\Delta\mu_i$ depends on the chemical composition of the material and is restricted to varying within the stability region of the chalcopyrite phase. The upper bound $\Delta\mu_i = 0$, corresponding to i-rich conditions, ensures that the elements do not precipitate into their elemental phases, while the lower bound marks the limit where competing phases such as $CuIn_5Se_8$ and Cu_3Se_2 start to form [24, 27].

According to Equation 3.6, the formation energy for charged defects ($q \neq 0$) depends on the Fermi level position within the band gap. In cases where a point defect may exist in several different charge states, the stable charge state at a specific value of Fermi level is the one having the lowest formation energy. A Fermi level position where the stable charge state changes spontaneously from q to q' is called a charge transition level $\epsilon(q/q')$. The charge transition levels computed from these total-energy differences can be compared to experimentally measured ionization levels. However, they should not be confused with the Kohn-Sham states obtained from band-structure calculations [61].

3.4.1 Finite-size corrections

The use of periodic boundary conditions for finite-sized supercells introduces an artificial interaction between the defect and its images in neighboring supercells. This interaction can result in both elastic and electrostatic effects, which contribute to the total energy of the system and essentially make defect energetics dependent on the supercell size used. Elastic effects arise when the supercell is not able to fully accommodate the relaxation around the defect. Electrostatic effects typically pertain to charged defects, which require a homogeneous neutralizing background charge to ensure that the electrostatic energy per unit cell remains finite [62]. In addition, the presence of a defect gives rise to a constant shift in the electrostatic potential of the supercell, which affects the position of the valence-band maximum in Equation 3.6. Other finite-size-related effects include defect level dispersions arising from the overlap of wavefunctions,

which distort ideally flat defect levels along k space.

If the supercell size would be increased sufficiently, all of these finite-size effects would essentially become negligible. Yet, in practice, feasible supercell sizes are limited by the available computational resources. Although finite-size errors converge rapidly with supercell size for charge-neutral defects, they remain significant for defects in high charge states [62]. Correcting for them is therefore indispensable in order to obtain qualitatively correct predictions about defect energetics.

Various correction schemes have been designed to address specific finite-size errors, most notably, the potential alignment scheme [61], Makov-Payne correction [44], and Freysoldt correction [63]. In principle, they have all been found to scale inversely linearly with the dimension L of the supercell and/or the cube L^3 [64, 65], reflecting the scaling behavior of elastic and electrostatic interactions. However, their direct application particularly to small supercells may sometimes result in unpredictable outcomes. For instance, the simultaneous application of the potential alignment and Makov-Payne corrections has led to double-counting of the linear term [65], while the Makov-Payne scheme on its own overestimates energies in some cases [66].

Rather than applying directly one or more energy corrections to a finite-sized supercell, the finite-size errors have been addressed with a finite-size-scaling extrapolation method [65] in this thesis, which consists of performing a series of calculations in differently-sized supercells and then extrapolating the formation energies to the dilute limit. The method follows the proven dependencies of the energy on the linear and cubic di-

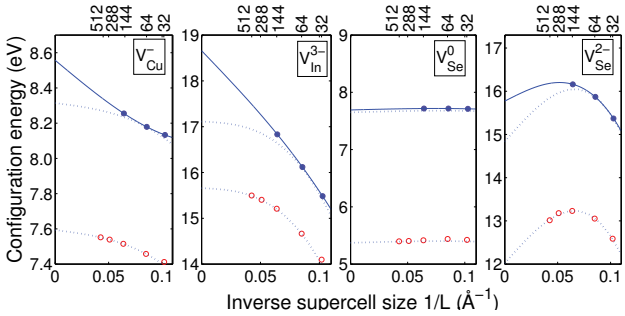

Figure 3.2. Convergence of configuration energies with respect to the inverse supercell size $1/L$ for the vacancies in CIS. A function of the form in Equation 3.7 has been fitted to the results. The values on top of the graphs denote the number of atoms per supercell. The red circles and blue dots represent values calculated with PBE-GGA and HSE06, respectively (from Publication IV).

mensions of the supercells, but includes the scaling coefficients as fitting parameters instead of predefined quantities:

$$E_{\text{conf}}(L) = E_{\text{conf}}(L \to \infty) + a_1 L^{-1} + a_3 L^{-3}, \tag{3.7}$$

where a_n and $E_{\text{conf}}(L \to \infty)$ are fitting parameters, $E_{\text{conf}}(L \to \infty)$ corresponding to the extrapolated configuration energy. In this thesis, the configuration energy $E_{\text{conf}} = E^q_{\text{defect}} - E_{\text{bulk}}$ has been used instead of the formation energy, E_f, in order to avoid defining E_{VBM} at each supercell size. After extrapolating E_{conf} to an infinitely large supercell, the value of E_{VBM} corresponds to that of an infinite crystal and can be taken from the bulk calculation. This removes the need for a separate potential alignment scheme. A similar procedure has been performed for binding energies. The procedure is illustrated in Figure 3.2. More details can be read from Publication IV.

3.4.2 Accuracy of calculations

Theorists often refrain from explicitly evaluating the accuracy of their calculations. The sources of error are commonly identified and the importance of addressing them somehow is widely accepted, but conclusions regarding the accuracy of the outcome are rarely discussed. Assigning error bars for computed values is indeed very problematic and at worst may seem arbitrary. On the other hand, leaving error bars out can be very misleading for experimentalists reading the reports, who might pick the reported values as they are and try to correlate them with their own findings without being fully aware of the broadness of uncertainty involved.

Sources of error can be commonly divided into two categories: internal and external. Regarding DFT calculations, internal errors would consist of errors arising from the (insufficient) convergence of calculation parameters – these errors could in principle be completely eliminated if accurate enough parameter values are used for the cutoff energy and k point sampling, along with an infinitely large supercell. In practice, the accuracy is ultimately limited by the available computational resources. In this thesis, error bars have been estimated based on studying the convergence of configuration energies and extrapolating them to the dilute limit. The error bars become substantial typically in the case of charged defects.

External errors concern the accuracy of the Kohn-Sham method itself, which is essentially determined by the choice of the exchange-correlation functional. Provided an unlimited supply of computational resources, how

far would the results still lie from experiment? In point defect calculations, a central issue is how well the computed band gap reproduces the experimental one since it not only describes the electronic and optical properties of the bulk material, but also strongly influences the accuracy of defect-related quantities such as charge transition levels and formation energies. Within (semi)local approximations, the Kohn-Sham band gap obtained as the energy difference between the highest occupied and lowest unoccupied orbitals is underestimated typically by 50% compared to the fundamental band gap due to the lack of derivative discontinuities as discussed in Section 3.2 [49]. Non-local exchange-correlation functionals, such as hybrid functionals, partly alleviate the error in the eigenvalues, thus opening up the gap [67]. It has even been suggested that, provided an appropriate choice of parameters, hybrid functionals could actually obey the generalized Koopmans theorem, implying that the correct piecewise linear behavior of the exchange-correlation functional would be recovered and that the Kohn-Sham eigenvalue of a defect would exactly equal its ionization energy [68].

In practical calculations employing hybrids or other gap-correcting methods such as LDA+U, the tunable parameters are often chosen to match the Kohn-Sham band gap with the experimental one. A comparison of hybrid-functional calculations with varying parameter values recommends the tuning, which resulted in an accuracy of 0.2 eV for the charge transition levels [69]. However, the success in reproducing band gaps does not automatically guarantee a decent description of all other material properties. Recently, the reliability of charge transition levels obtained from hybrid-functional calculations was demonstrated to depend not on the Kohn-Sham gap width, but instead on the upper valence-band width, which reflects how well binding is described within the system [70]. This suggests that the most obvious choices for parametrization may not find full justification from the underlying physics after all.

4. Results

4.1 Formation energies: Which point defects exist in CIS?

When characterizing the microstructure of a semiconductor material, the first and foremost task is to determine which point defects can exist there in substantial quantities. Point defects govern several important material properties, such as electronic properties, and also play a key role in mediating mass transport during material growth and processing. In this Section, the formation energies of likely point defects in CIS are explored in order to obtain a first impression on its defect structure. These results have been presented in Publications I, IV, and V.

CIS crystallizes in the chalcopyrite structure, which is derived from the zincblende structure by occupying cation sites alternatingly with copper and indium atoms. The chalcopyrite lattice may sustain twelve different kinds of intrinsic point defects, which can be vacancies, interstitials, or antisites (see Figure 4.1). In addition, foreign dopants and impurities may get incorporated to the lattice during material growth and processing, creating extrinsic point defects in the material. By tuning the concentrations of all these defects, the electronic properties of the material can be modified in a process called doping. Unlike in other, more conventional semiconductors, intrinsic defects in CIS provide alone a sufficient concentration of charge carriers for device operation, making the material natively doped. However, it has been experimentally observed that the addition of small amounts of sodium further enhances the electronic performance of CIS-based solar cells. In this work, both intrinsic and sodium-related point defects are therefore considered.

The formation energies of relevant point defects in CIS are presented in Figure 4.2 as a function of the Fermi level position. The range of Fermi

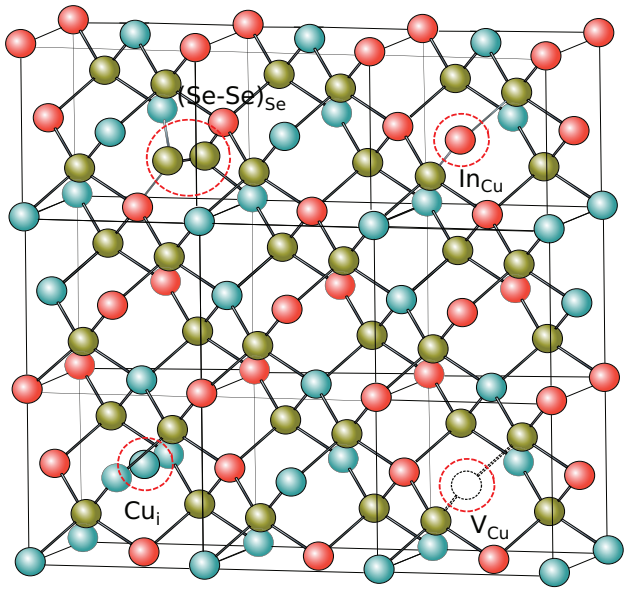

Figure 4.1. Schematic illustration of selected point defect configurations in the CIS chalcopyrite lattice: V_{Cu}, Cu_i (octahedral site), $\mathrm{In}_{\mathrm{Cu}}$, and $(\mathrm{Se\text{-}Se})_{\mathrm{Se}}$. Copper atoms are denoted in blue, indium atoms in red, and selenium atoms in green.

energy extends from the calculated VBM (corresponding to 0 eV) up to the experimental band gap (1.04 eV). The formation energies have been computed with Equation 3.6 after finite-size-scaling extrapolation as described in Section 3.4.1. Finite-size scaling is crucial to take into account since the error in the formation energy computed in a 64-atom supercell, for instance, can be several tenths of eV for a defect in the $1-$ charge state and much larger, even of the order of eV, for defects in higher charge states. The extrapolation itself leads to some uncertainties, which are expressed as error bars in the side panel in Figure 4.2.

Figure 4.2 shows that most of the considered intrinsic defects are stable in only one charge state and do not create charge transition levels within the band gap. In each case, the stable charge state can be deduced from the slope of the linear function in accordance with Equation 3.6. The stable charge states find correspondence from the Kohn-Sham band structures, which should be evaluated to gain an understanding of the electronic behavior of each defect (see Section 4.4).

Among these intrinsic defects, copper-related defects such as V_{Cu}, $\mathrm{Cu}_{\mathrm{In}}$, $\mathrm{In}_{\mathrm{Cu}}$, and Cu_i stand out as the most prominent ones under most chemical conditions. Copper vacancy has a particularly low formation energy, which can even reach zero under copper-poor conditions. This point marks

the so-called Fermi pinning level where copper vacancies start to form spontaneously and compensate any attempt to further elevate the electron doping level. Likewise, the formation energies of $\mathrm{In_{Cu}}$ and $\mathrm{Cu_{In}}$ antisites remain below about 2 eV under most chemical conditions and may fall to zero at both doping extremes of the material. Additional copper atoms, interstitials, are also easily accommodated into the lattice compared to other types of interstitials. In contrast, the formation of indium defects, V_{In} and In_i, is suppressed due to their mostly very elevated for-

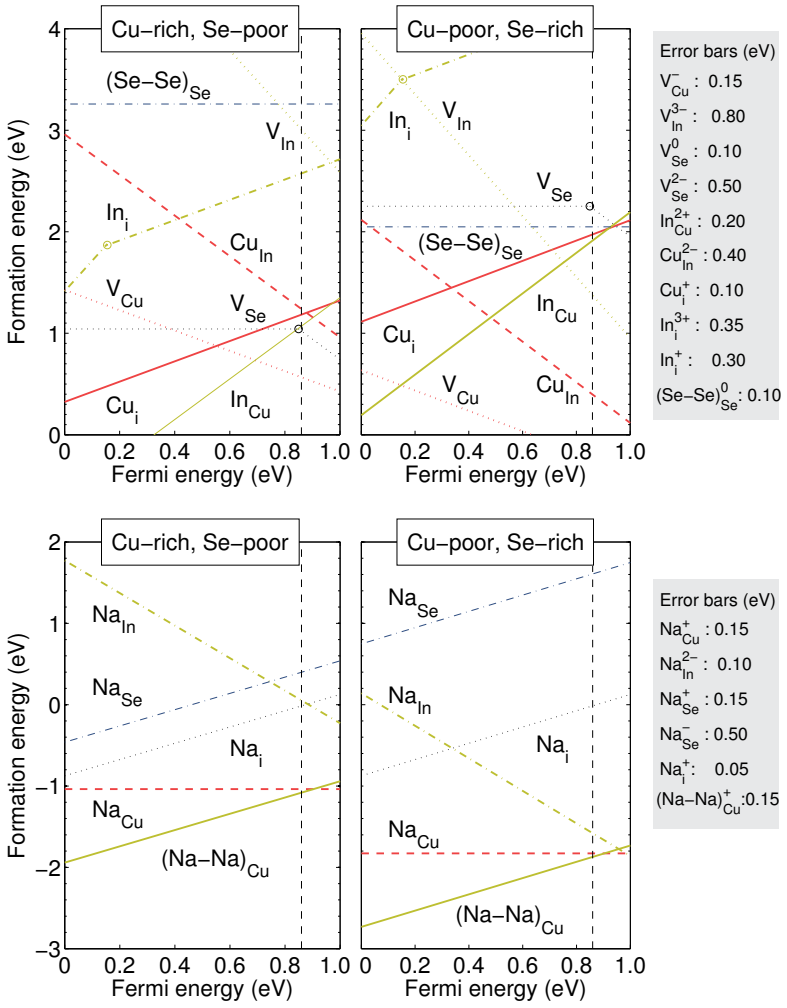

Figure 4.2. Formation energies of native point defects (upper panel) and Na-related defects (lower panel) in CIS as a function of Fermi level position. At the copper-rich limit, the corresponding chemical potentials for In and Se are $\Delta\mu_{\mathrm{In}} = 0$ eV and $\Delta\mu_{\mathrm{Se}} = -1.21$ eV. At the copper-poor limit, the chemical potentials are $\Delta\mu_{\mathrm{Cu}} = -0.79$ eV, $\Delta\mu_{\mathrm{In}} = -1.63$ eV, and $\Delta\mu_{\mathrm{Se}} = 0$ eV. The dashed line marks the band gap obtained with HSE06.

mation energies. All of these defects are structurally characterized by an isotropic relaxation, whose magnitude depends on the nature of the defect.

Selenium defects, V_{Se} and (Se-Se)$_{\mathrm{Se}}$, exist predominantly in the neutral charge state, maintaining constant formation energies almost throughout the Fermi energy range. They affect their atomic surroundings very differently than the typical cationic defects both from the electronic and structural points of view. V_{Se} induces a transition level $\epsilon(0/2-)$ at 0.85 $\pm$ 0.20 eV above the VBM and may thus act as an electron trap, whereas the selenium dumbbell, depending on its orientation, may induce a defect level slightly above the VBM and may thus participate in p-type conductivity. Regarding structural factors, the removal of a selenium atom leads to strong anisotropic elastic relaxation with the nearest-neighbor indium atoms forming a bond while the copper atoms are pushed away from each other. This relaxation becomes stronger when the charge state of V_{Se} changes from 0 to $2-$. The lowest-energy configuration for an extra selenium atom is a dumbbell configuration, where it pairs up with a lattice selenium atom. Although additional copper and indium atoms could also form dumbbell structures, they are local minimum-energy states surrounded by very low barriers and can therefore dissociate very easily.

Introducing sodium into CIS creates additional defects in the lattice. As shown in Figure 4.2, Na prefers to occupy a copper site, either forming Na$_{\mathrm{Cu}}$ or even a (Na-Na)$_{\mathrm{Cu}}$ dumbbell whenever there are vacant copper lattice sites available. Under copper-rich conditions, Na may either stay as an interstitial or replace a lattice copper atom. The formation of Na$_{\mathrm{In}}$ or Na$_{\mathrm{Se}}$ defects is not favored due to their relatively high formation energies. It should be noted that in the case of extrinsic defects, the thermal formation energies cannot be used as an absolute measure of defect quantities since the actual sodium concentration in CIS is not determined by thermal concentration but rather by external conditions such as growth.

4.2 Diffusion kinetics: How do point defects migrate in CIS?

Instead of holding still, vacancies and interstitials are constantly exchanging sites with lattice atoms, jumping in between them, and diffusing around the crystal lattice. Defect diffusion not only leads to a redistribution of the defects themselves, with part of them agglomerating into clusters, but it also mediates mass transport starting from film growth and persisting

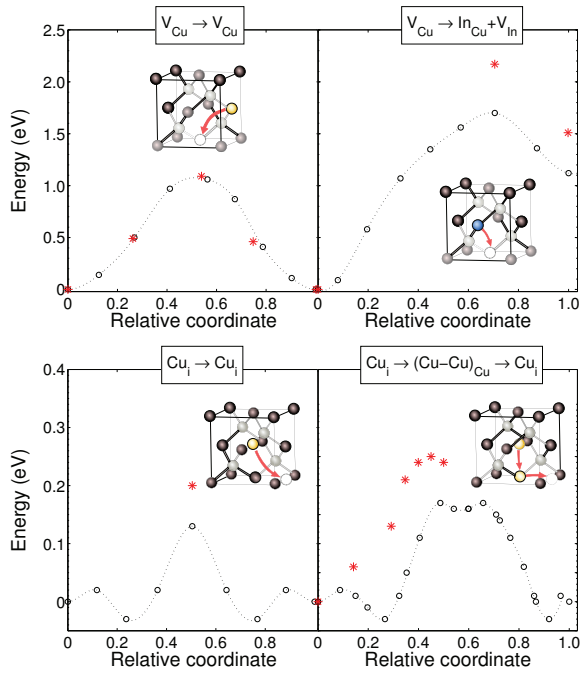

Figure 4.3. Migration paths for copper vacancy (upper panel) and copper interstitial (lower panel) in CIS. The diffusing copper atoms are drawn in yellow and indium atom in blue. The red stars and open circles represent values calculated with HSE06 and PBE-GGA, respectively. The dotted lines are guides to the eye. For clarity, only one-eighth of the 64-atom supercell is displayed in the schematic figures (from Publication IV).

during device operation. In this Section, the fastest-diffusing defects in CIS are identified, and their role as mass-mediating agents is considered. These results have been presented in Publications III and IV.

The viable diffusion jumps in a lattice can be modelled with the climbing-image nudged-elastic-band (CINEB) method [71], which outlines the minimum-energy path between given initial and final states. The climbing-image algorithm makes sure that the saddle point of the path is reached. The energy barrier faced by each defect is then calculated as the energy difference between the saddle-point and lowest-energy configurations. Within the lattice structure, jumps can terminate at the first-nearest-neighbor (1NN) shell or extend over longer distances. In this work, jumps to the 1NN and 2NN shells have been considered for the vacancies and between two equivalent lattice sites for the interstitials. In both cases, jumps may result in the creation of antisites if the jumping defect is transferred into another sublattice.

Besides these energy barriers, the rate of atomic diffusion depends on

the formation energy of the mediating defect in thermal equilibrium. The sum of these two terms, the activation energy, can be used to evaluate the magnitudes of distinct diffusion mechanisms under different chemical conditions. For each elemental component of CIS, self-diffusivity is a competition between vacancy-mediated and interstitial-mediated processes, one of them dominating in each compositional regime. The leading mechanism for each component may also vary depending on temperature, but it was not found to be affected in typical growth and processing temperatures in this work.

Of the three components forming CIS, copper is found to be the fastest diffusing element. Both of its mass-mediating agents, V_{Cu} and Cu_i, exist in the material abundantly and face rather low energy barriers of 1.09 and 0.22 eV, respectively (see Figure 4.3). Copper interstitials mediate mass transport under copper-rich conditions. Under copper-poor conditions, mass transport occurs via interstitials up to Fermi level position of 0.2 eV and via copper vacancies at higher electron doping levels.

Likewise, selenium mass transport is sensitive to the stoichiometry of the material. Under selenium-rich conditions, selenium mass transport relies solely on $(\mathrm{Se\text{-}Se})_{\mathrm{Se}}$ dumbbells, which diffuse with a barrier of 0.24 eV. Under selenium-poor conditions, a competition takes place between the dumbbells and selenium vacancies, whose diffusion is hindered by a migration barrier of 2.19 eV. Selenium dumbbell, in particular, experiences a very diverse potential energy surface, and its diffusion path is much more complicated than for any other considered defect. Selenium diffusion requires higher temperatures than copper to become feasible since its activation barriers are greater.

Surprisingly, indium plays no role in long-range mass transport in CIS; instead, indium vacancies and interstitials participate in mechanisms that promote the formation of antisites in the cation sublattice. V_{In} would rather jump to the 2NN copper site, forming $\mathrm{Cu}_{\mathrm{In}}$-$V_{\mathrm{Cu}}$ (activation barrier of 0.70 eV) than to exchange sites with an indium atom (1.00 eV). In_i, for its part, will always kick out a copper atom into an interstitial site, forming $\mathrm{In}_{\mathrm{Cu}}$-$\mathrm{Cu}_i$ provided it overcomes a barrier of 0.28 eV. The role of these indium-related processes is, however, diminished by the negligible thermal concentrations of indium defects.

4.3 Defect interactions: Which kinds of complexes can point defects form in CIS?

In the previous Section, the migration jumps of individual defects were considered in an infinite crystal. However, in real crystals, the potential energy surface experienced by a defect can be modified by the nearby presence of other defects. For instance, a defect may get trapped by another defect through an attractive potential, leading to the formation of a defect complex. These phenomena are controlled by temperature and result in constant formation and dissociation processes even at room temperature. In this Section, the thermodynamic and kinetic factors behind defect complex formation and dissociation in CIS are evaluated. These results have been presented in Publications IV (native defects) and V (sodium).

In addition to being thermally formed, defect complexes can be frozen in already during material growth and processing, or alternatively can be created as a result of monodefects diffusing and binding together. Film growth conditions typically remain far from equilibrium, and the following equilibration of microstructure is limited by atomic diffusion. Defects and complexes frozen in may therefore give a substantial contribution to defect concentrations. Their stability against thermal dissocation determines the time interval when they can be expected to affect the material properties. In this thesis, these processes are considered for $\mathrm{In_{Cu}}$-$2V_{\mathrm{Cu}}$, $\mathrm{Cu_{In}}$-$\mathrm{In_{Cu}}$, V_{Se}-V_{Cu}, and V_{Se}-$2V_{\mathrm{Cu}}$.

Except for the antisite pair, a common denominator for all the considered complexes is copper vacancy. As was demonstrated in Section 4.2, copper vacancy is able to diffuse fairly easily in the material compared to other point defects, and thus it can promote the kinetic formation of V_{Cu}-related complexes. The interaction potentials for each pair or triplet are plotted at different separations as they are approaching each other in Figure 4.4. The defect triplets have been considered to form in two steps, with two defects first binding together, followed by a third defect.

In each case shown in Figure 4.4, the binding energy grows rather smoothly when the defects are brought closer together and reaches its maximum when they occupy nearest-neighbor (1NN) sites. Complex formation is thus clearly favored over an infinite separation of the defects, with binding energies in the range of 0.19-0.30 eV in V_{Cu}-related defects and amounting to 0.70 eV in the antisite pair. The separation at which the binding energy starts to increase from zero, i.e. the defects become aware of each

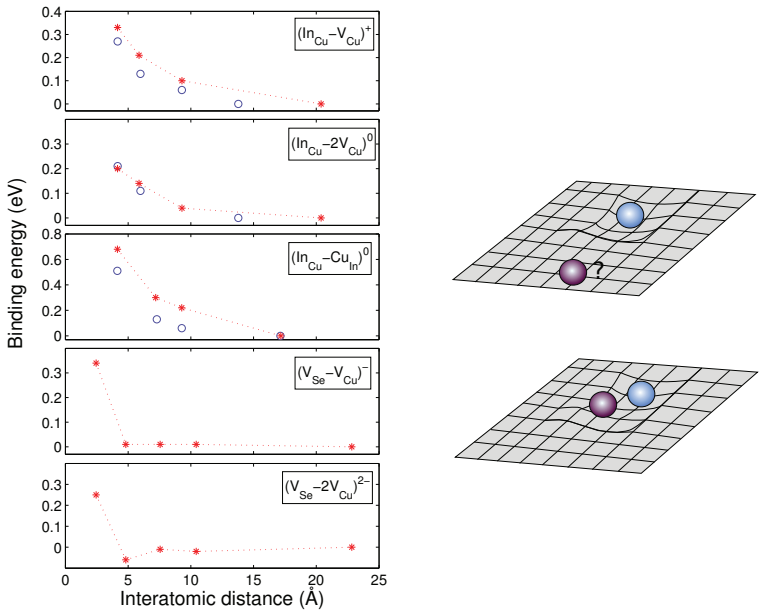

Figure 4.4. Left panel: Binding energies at different separations between defects. In each case, the interatomic distance has been determined as the minimum separation between the defect (pair) and the displaced defect. The blue circles and red dots represent PBE-GGA calculations in 144- and 512-atom supercells, respectively. The lines are guides to the eye (from Publication IV). Right panel: Schematic illustration of how the potential energy surface experienced by a defect is altered by the nearby presence of another defect.

other, can be considered a capture radius inside of which defects can trap each other. The capture radius is rather long, spanning several lattice constants, for $\mathrm{In_{Cu}}$-V_{Cu} and $\mathrm{In_{Cu}}$-$2V_{\mathrm{Cu}}$, whereas it is much shorter for vacancy pairs and triplets. Overall, there exists a thermodynamic driving force for the creation of these defect complexes in CIS, which sets in much earlier in complexes involving $\mathrm{In_{Cu}}$ than in vacancy complexes. Part of the driving force probably stems from electrostatic attraction since the complexes with highest binding energies are oppositely charged – indeed, $\mathrm{In_{Cu}}$ and $\mathrm{Cu_{In}}$ exhibit charge states of $2+$ and $2-$, respectively. Elastic relaxation can also play a role in favoring complex formation, as with $\mathrm{In_{Cu}}$-V_{Cu}, whose elastic relaxation is not fully accommodated in a small supercell and becomes stronger with the increase of the supercell size.

Together, the binding energy at 1NN configuration and the migration barriers surrounding the complex determine the dissociation energy, that is, its stability against thermal dissociation. For the considered complexes, contributions from binding energies are relatively small, mostly

0.2-0.3 eV, which do not indicate particular stability by themselves. Yet adding up the migration barrier of V_{Cu}, 1.09 eV, results in dissociation energies in the range of 1.3-1.4 eV. Therefore, the considered complexes will not dissociate frequently at device operating temperatures once formed or frozen in.

In order for complex formation to occur, the binding energy can actually be negligible provided that the barrier for jumping away is large enough. This is the case if Na is introduced into CIS. Na prefers to occupy copper sites, forming $\mathrm{Na}_{\mathrm{Cu}}$. This substitutional defect can capture a copper vacancy based on kinetics: though the complex $\mathrm{Na}_{\mathrm{Cu}}$-$V_{\mathrm{Cu}}$ has a vanishing binding energy, the barrier for exchanging places between V_{Cu} and $\mathrm{Na}_{\mathrm{Cu}}$ amounts to only 0.35 eV compared to V_{Cu} jumping off with 1.09 eV. Therefore, these two defects will form a dynamically stable complex: it is energetically much less costly for V_{Cu} to jump back and forth with the antisite than to jump away in the opposite direction. More broadly speaking, this will also reduce copper diffusion in CIS in the presence of Na.

4.4 Band structures: How do point defects modify the electronic properties of CIS?

Point defects typically induce defect levels within the band gap of the host material, thereby altering its electronic properties. The effect on the electronic structure can depend on whether the defect stays isolated or is part of a defect complex. Defect levels also provide an important measure when identifying point defects experimentally. In this Section, defect-induced levels are examined in CIS and it is shown that recombination centers in this material arise from selenium-related point defects. These results have been presented in Publications II and IV.

A first impression of the electronic effect of a defect on the host material can be obtained by computing the corresponding Kohn-Sham band structure in a few different charge states and carefully studying whether defect-induced levels appear there. While, strictly speaking, the Kohn-Sham eigenvalues are not one-electron energies and thus cannot be directly compared to experimental spectra, they still provide an important qualitative view of the electronic levels. A defect-induced level lying within the Kohn-Sham band gap region is a necessary though not sufficient condition for a transition between two charge states to take place. Therefore, if no defect-induced single-particle levels appear in the band gap region

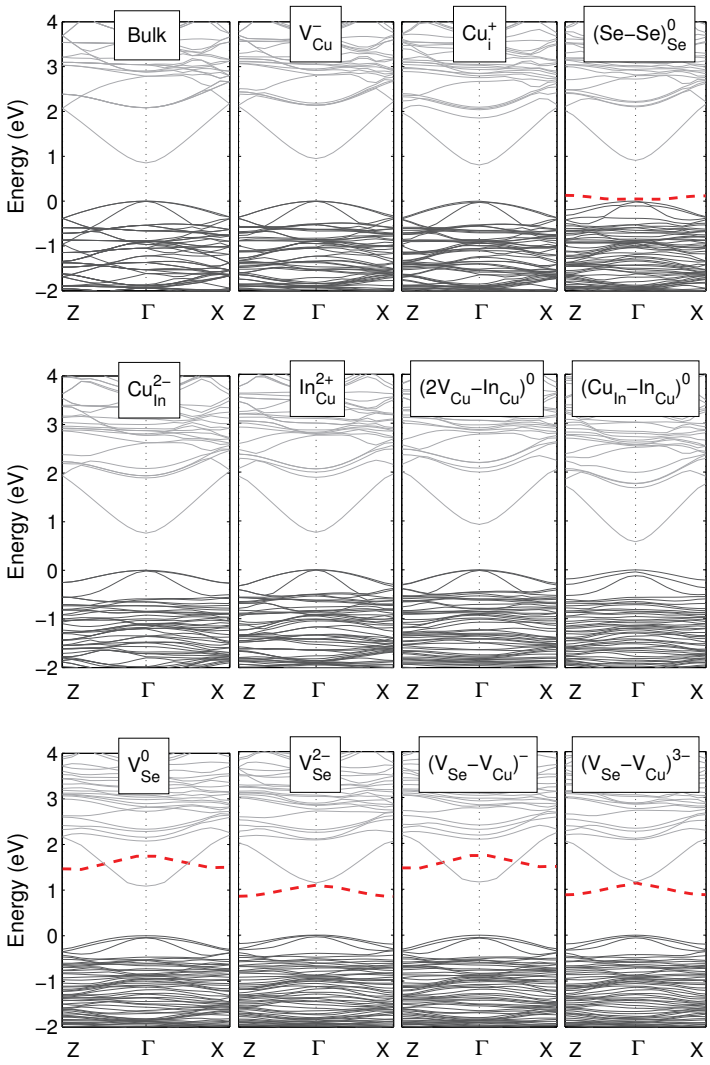

Figure 4.5. Kohn-Sham band structures for bulk CIS and selected point defects. The occupied levels are drawn in dark grey and the unoccupied levels in light grey. The dashed lines illustrate the defect-induced levels compared to the bulk band structure in each case.

in any charge state – while acknowledging the extent to which finite-size effects may displace defect levels – it can be concluded that the defect will remain stable in only one charge state and not have transition levels within the gap. The quantitative values for charge transition levels must be calculated from total-energy differences as has been done in Section 4.1.

The Kohn-Sham band structures corresponding to selected prevalent point defects in CIS are presented in Figure 4.5. Regarding the cation defects located in the cation sublattice, it can be clearly seen that none of them yields single-particle levels in or near the band gap. Each of these defects can therefore exist in only one charge state corresponding to the fully occupied valence band.

In contrast to these cationic defects, selenium-related defects induce single-particle defect levels within the CIS band gap. This indicates that they can exist in multiple charge states. When the levels are filled only up to the VBM, unoccupied defect level(s) located in the upper part of the gap may hybridize with the lowest conduction-band states. The addition of electrons is typically accompanied by strong lattice relaxation and single-particle defect levels shifting downwards in the band gap region, as depicted for V_{Se} in Figure 4.5. The selenium-related defects are likely to act as recombination centers in the material, and particular attention should be paid to them when attempting to reduce charge carrier recombination in CIS.

According to Figure 4.5, the Kohn-Sham band structures of the considered defect complexes seem to retain the characteristics of the isolated defects. When a cationic monodefect (such as V_{Cu} or $\mathrm{In}_{\mathrm{Cu}}$) has no single-particle levels within the gap, bringing two or more cationic defects together (such as $\mathrm{In}_{\mathrm{Cu}}$-$2V_{\mathrm{Cu}}$) does not affect the electronic properties of the material. Similarly, complexes involving a selenium-related defect such as V_{Se} display the same features as the isolated selenium defect as in the case of V_{Se}-V_{Cu} and V_{Se}-$2V_{\mathrm{Cu}}$. Yet the formation of a charge-neutral complex passivates the possibly electrically active monodefects.

5. Discussion and outlook

5.1 Critical evaluation of exchange-correlation functionals

Despite the success of DFT in describing and predicting material properties, the outcome of the calculations often remains sensitive to the choice of the exchange-correlation functional. The most widely used functional, LDA, is known to underestimate semiconductor band gaps, which leads to broad uncertainty ranges for various defect-related quantities. The hybrid functional HSE06 employed in this thesis has been shown to provide an improved description of structural and electronic properties. Besides the exchange-correlation functional, the accuracy of the calculations also depends on how the finite-size effects arising from the limited supercell size are addressed. In the following, the reliability of the present results is assessed and compared to previously reported LDA results.

One of the most fundamental quantities in point defect calculations is the formation energy. In the case of a defect in a charge state corresponding to a fully occupied valence band, the formation energy is often assumed to be a ground-state property that should be well described even with (semi)local functionals [72]. However, this should not always be taken for granted [73]. Moreover, when the defect involves occupied gap levels, the computation of its formation energy will face similar problems as when trying to calculate excitation energies starting from a ground-state theory [2]. Therefore, switching to a hybrid functional, which opens up the gap, can be expected to improve the formation energy values compared to (semi)local functionals. It turns out that HSE06 generally increases the formation energies of negatively charged defects and decreases those of positively charged defects – this has been attributed to a lowering of the VBM, which is used as the reference point when computing forma-

tion energy values [2, 74]. The change in the position of the VBM – when aligned to the average local potential – signifies that HSE06 corrects, in part, the self-interaction error inherent in (semi)local functionals. Often, however, the reported values do not only reflect the functional used, but also various *a posteriori* corrections that have sometimes been used on top of each other, thus complicating direct comparison between different studies. This being said, the results presented in this work mostly validate the relative magnitudes of the defect formation energies obtained in previous studies [22, 24, 30, 32]. In particular, the role of copper-related defects has been emphasized in all works. An exception is Cu_i, which based on the first DFT calculations employing LDA was shown to have a high formation energy and thus its existence was dismissed [24], until recently its role was reconsidered based on HSE06 calculations [21].

In calculating formation energies, a critical step comes from the choice of elemental chemical potentials. The first defect calculations in CIS employed atomic chemical potentials [23]. This was later criticized in [24], where the current standard procedure was set to using metallic chemical potentials instead. Yet even employing the same procedure does not guarantee uniform outcomes as exchange-correlation functionals differ in how well they describe the energetics of different elements. HSE06 performs well overall and, for instance, improves the description of indium and selenium atomization energies compared to semilocal PBE-GGA. Meanwhile, HSE06 is known to fail in the description of transition metals [75]. In this thesis, the atomization energy of fcc copper computed with HSE06 is found to be underestimated by 0.44 eV compared to experiment, whereas GGA-PBE is able to reproduce the experimental value remarkably well. This deficiency may result in an overestimation (underestimation) of defect formation energies involving a removal (addition) of a copper atom.

Compared to formation energies, quantities computed from energy differences between two defect configurations, such as migration barriers and binding energies, should be less susceptible to the choice of exchange-correlation functional due to the cancellation of various terms and may therefore be considered to be more reliable. Indeed, the results in this thesis show that the agreement between PBE-GGA and HSE06 in this respect is very good. Yet this outcome may not reflect a general trend between the two functionals. Rather, it can stem from the fact that these configurations do not involve occupied defect levels within the band gap but correspond to fully occupied valence bands [73]. The migration barrier

values computed with either functional stay mostly the same – the only major differences arise when the diffusion path shows marked complexity or when the functionals give a different ordering of energetic preference between different configurations. For instance, the energy minimum for Cu_i is reached at the trigonal site with PBE-GGA and at the octahedral site with HSE06. Moreover, the diffusion jump of In_i is qualitatively different depending on the functional used: it can only go to take over a copper site with HSE06, while PBE-GGA allows jumps from one equivalent site to the next one. Regarding binding energies in this thesis, they are practically not affected by the choice of exchange-correlation functional. Yet, it is demonstrated that binding energies depend strongly on the supercell size, similar to formation energies, and that this effect must be taken into account to obtain qualitatively correct descriptions of defect interactions, such as whether two defects attract or repel each other.

The most widely recognized problem of point defect calculations within DFT is that they do not allow relating experimentally observed ionization levels to specific defects with a high level of confidence. As a matter of fact, disagreement over stable charge states and ionization levels also persists within the theoretical community. This problem reflects in part the band gap underestimation, finite-size effects, correction schemes employed for these two deficiencies, and how the results are interpreted in the end. Zunger's group has assigned at least one transition level for each point defect in CIS, bringing forth V_{Cu} as the dominant acceptor-type defect [24, 30] and $\mathrm{In}_{\mathrm{Cu}}$ as the main donor [27]. In contrast, by studying Kohn-Sham band structures in this thesis, it is concluded that the prevalent cationic defects do not create defect-induced levels within the CIS band gap, thereby sustaining only one stable charge state each. It is suggested that the levels reported by Zunger arise from occupying extended bulk states near the VBM or CBM instead of defect-induced ones. Though these defects could, in principle, also create hydrogenic effective-mass-like states [76, 77], this can be neither confirmed nor rejected by the current status of DFT calculations. Moreover, the errors involved in the present calculations are invariably larger than the distance of the suspected defect levels from the band edges. Speculations on the topic are therefore intentionally restrained in this thesis.

Overall, although HSE06 has brought a least a partial resolution to the band gap problem, one step has been taken back due to computational restrictions on the supercell size. The finite supercell size basically af-

fects all defect-related properties: formation energies, migration, binding, and – most severely – charge transition levels. While all of these can be corrected to a decent degree of accuracy by extrapolating to the dilute limit, the question about effective-mass-like states persists. Recently, another approach combining DFT and GW aimed at resolving this issue by employing a staggering supercell of 64 000 atoms [78]. Routine calculations of this size remain, however, far from the present status of computations, and reported results on point defect calculations should be evaluated keeping in mind the associated error bars though they are often not explicitly shown. In any case, there is no doubt that point defects in CIS would be play important roles when reaching for optimal solar cell performance or that theoretical calculations have so far provided invaluable support for the understanding of these effects.

5.2 Practical implications

In this thesis, point defects in the solar cell absorber material $CuInSe_2$ (CIS) have been investigated with density-functional theory employing a hybrid exchange-correlation functional. Point defects such as vacancies, antisites, and interstitials as well as impurities are a determining factor for the conversion efficiency of a thin-film solar cell by controlling doping but also by degrading device performance. Additionally, point defects play a role in material growth and processing by mediating diffusion. The aim of the thesis was therefore to gain a comprehensive understanding of the defect behavior and its effect on the electronic properties of the material, which would benefit the systematic development of CIS-based solar cells towards greater conversion efficiencies.

CIS is known to tolerate large compositional inhomogeneities and exhibits a variety of point defects. Both prior and present theoretical calculations agree on the most prominent point defects in CIS, most importantly, V_{Cu}, $\mathrm{In}_{\mathrm{Cu}}$, and $\mathrm{Cu}_{\mathrm{In}}$. The observed off-stoichiometry in CIS and its tendency to copper-poorness may thus be at least partly explained by the abundance of copper vacancies and the mixing of atomic species in the cation sublattice. In this thesis, it is shown that even cationic antisite pairs may arise in CIS provided that they are formed already during film growth followed by fast cooldown. Further, mechanisms promoting the kinetic formation of cationic antisites are identified, which at the same time suppress the mass transport of indium.

Though indium diffusion is shown to be negligible, the other two components of CIS may diffuse. It is demonstrated that diffusion mediated by copper vacancies and interstitials make copper the most mobile species in the compound, validating experimental observations [79, 80]. Selenium diffusion is led either solely by selenium dumbbells or dumbbells together with selenium vacancies depending on chemical conditions. In actual CIS samples, grain boundaries are also expected to play an important role in defect diffusion.

Based on studying defect interactions, it is shown that there exists a thermodynamic driving force towards the creation of specific defect complexes. Indeed, most of the prominent point defects may take part in complexes such as $\mathrm{In_{Cu}}$-$2V_{\mathrm{Cu}}$ and V_{Se}-V_{Cu}. The formation of charge-neutral complexes in CIS has been previously invoked several times to explain the discrepancy between experimentally measured charge carrier and defect concentrations [81, 82], the tolerance to off-stoichiometry, as well as the creation of ordered-vacancy compounds [24], but has never been properly validated until now.

Interaction of intrinsic defects with impurities can lead to surprising effects: it is found that by introducing sodium atoms into CIS, copper mass transport is reduced due to the capture of copper vacancies by $\mathrm{Na_{Cu}}$ defects. This finding provides an explanation for the experimental observation of sodium reducing copper diffusion at low substrate temperatures [83]. This mechanism should also affect the defect distribution within the material, including a decrease in the concentrations of other V_{Cu}-related complexes following the reduction in available copper vacancies. These atomic-scale rearrangements could be one reason behind the experimentally demonstrated improvement of the performance of CIS-based solar cells with the incorporation of sodium (see Refs. [5, 84] and references therein).

The effect of a point defect or defect complex on the electronic properties of CIS is found to essentially depend on whether the defect is of cationic or anionic type. Among the prevalent point defects in CIS, only selenium-related anionic defects are observed to create deep defect levels within the band gap, implying that they may act as recombination centers. This finding should be taken into account when attempting to reduce charge carrier recombination in the bulk, which is the main type of carrier loss mechanism in copper-poor CIS-based solar cells [85, 86, 87].

This thesis unravels several competing atomic-scale processes affecting

the defect distribution within CIS. However, having all of the mechanisms operating simultaneously, it is very difficult to tell *a priori* which of them would be dominant in determining the observed properties of the material. This question could be studied further by performing kinetic Monte Carlo simulations starting from all the values obtained in this work given as input.

The results presented in this thesis outline a view of the defect microstructure in CIS from a computational perspective, examining atomic-scale phenomena such as mass transport and defect clustering that remain practically out of reach in experiments. These findings can be used in gaining control over the CIS material growth process, and ultimately, film quality and device operation. Furthermore, the thesis provides a comprehensive theoretical framework for studying the microstructure formation in a three-component compound.

Bibliography

[1] R. J. D. Tilley. *Defects in Solids*. John Wiley & Sons, 2008.

[2] C. G. Van de Walle and A. Janotti. Advances in Electronic Structure Methods for Defects and Impurities in Solids. In *Advanced Calculations for Defects in Materials*. Wiley-VCH, 2011.

[3] R. M. Martin. *Electronic Structure: Basic Theory and Prcatical Methods*. Cambridge University Press, 2008.

[4] P. Jackson, D. Hariskos, E. Lotter, S. Paetel, R. Wuerz, R. Menner, W. Wischmann, and M. Powalla. New world record efficiency for Cu(In,Ga)Se_2 thin-film solar cells beyond 20%. *Prog. Photovolt. Res. Appl.*, 19(7):894–897, 2011.

[5] U. Rau and H.-W. Schock. Electronic properties of Cu(In,Ga)Se_2 heterojunction solar cells – recent achievements, current understanding, and future challenges. *Appl. Phys. A*, 69(2):131–147, 1999.

[6] S. Siebentritt, M. Igalson, C. Persson, and S. Lany. The electronic structure of chalcopyrites – bands, point defects and grain boundaries. *Prog. Photovolt. Res. Appl.*, 18:390–410, 2010.

[7] A. Bauknecht, S. Siebentritt, J. Albert, and M. Lux-Steiner. Radiative recombination via intrinsic defects in $Cu_xGa_ySe_2$. *J. Appl. Phys.*, 89:4391–4400, 2001.

[8] S. Siebentritt, N. Rega, A. Zajogin, and M. Lux-Steiner. Do we really need another PL study of $CuInSe_2$? *Phys. Stat. Sol. C*, 1:2304–2310, 2004.

[9] S. Siebentritt, I. Beckers, T. Riemann, J. Christen, A. Hoffmann, and M. Dworzak. Reconciliation of luminescence and Hall measurements on the ternary semiconductor $CuGaSe_2$. *Appl. Phys. Lett.*, 86:091909, 2005.

[10] M. Turcu, I. Kötschau, and U. Rau. Composition dependence of defect energies and band alignments in the Cu($In_{1-x}Ga_x$)($Se_{1-y}S_y$)$_2$ alloy system. *J. Appl. Phys.*, 91:1391–1399, 2002.

[11] J. T. Heath, J. D. Cohen, W. N. Shafarman, D. X. Liao, and A. A. Rockett. Effect of Ga content on defect states in $CuIn_{1-x}Ga_xSe_2$ photovoltaic devices. *Appl. Phys. Lett.*, 80:4540, 2002.

[12] T. Eisenbarth, T. Unold, R. Caballero, C. A. Kaufmann, and H.-W. Schock. Interpretation of admittance, capacitance-voltage, and current-voltage signatures in Cu(In,Ga)Se_2 thin film solar cells. *J. Appl. Phys.*, 107:034509, 2010.

[13] U. Reislöhner, H. Metzner, and C. Ronning. Hopping conduction observed in thermal admittance spectroscopy. *Phys. Rev. Lett.*, 104:226403, 2010.

[14] A. Polity, R. Krause-Rehberg, T. E. M. Staab, M. J. Puska, J. Klais, H. J. Möller, and B. K. Meyer. Study of defects in electron irradiated $CuInSe_2$ by positron lifetime spectroscopy. *J. Appl. Phys.*, 83(1):71–78, 1998.

[15] N. Nancheva, P. Docheva, N. Djourelov, and M. Balcheva. Positron and X-ray diffraction study of Cu-Se, In-Se and $CuInSe_2$ thin films. *Mater. Lett.*, 54(2-3):169–174, 2002.

[16] E. Korhonen, K. Kuitunen, F. Tuomisto, A. Urbaniak, M. Igalson, J. Larsen, L. Guetay, S. Siebentritt, and Y. Tomm. Vacancy defects in epitaxial thin film $CuGaSe_2$ and $CuInSe_2$. *Phys. Rev. B*, 86(6), 2012.

[17] M. M. Islam, A. Uedono, T. Sakurai, A. Yamada, S. Ishizuka, K. Matsubara, S. Niki, and A. Akimoto. Impact of Se flux on the defect formation in polycrystalline Cu(In,Ga)Se_2 thin films grown by three stage evaporation process. *J. Appl. Phys.*, 113:064907, 2013.

[18] I. Lubomirsky, K. Gartsman, and D. Cohen. Space charge effects on dopant diffusion coefficient measurements in semiconductors. *J. Appl. Phys.*, 83:4678, 1998.

[19] J. Pohl and K. Albe. Thermodynamics and kinetics of the copper vacancy in $CuInSe_2$, $CuGaSe_2$, $CuInS_2$ and $CuGaS_2$ from screened-exchange hybrid density functional theory. *J. Appl. Phys.*, 108:023509, 2010.

[20] J. Pohl and K. Albe. Errata: Thermodynamics and kinetics of the copper vacancy in $CuInSe_2$, $CuGaSe_2$, $CuInS_2$, and $CuGaS_2$ from screened-exchange hybrid density functional theory. *J. Appl. Phys.*, 110(10), 2011.

[21] J. Pohl, A. Klein, and K. Albe. Role of copper interstitials in $CuInSe_2$: First-principles calculations. *Phys. Rev. B*, 84(12), 2011.

[22] J. Pohl and K. Albe. Intrinsic point defects in $CuInSe_2$ and $CuGaSe_2$ as seen via screened-exchange hybrid density functional theory. *Phys. Rev. B*, 87:245203, 2013.

[23] H. Neumann. Vacancy formation enthalpies in $A^I B^{III} C_2^{VI}$ chalcopyrite semiconductors. *Cryst. Res. Techn.*, 18(7):901–906, 1983.

[24] S. B. Zhang, S.-H. Wei, A. Zunger, and H. Katayama-Yoshida. Defect physics of the $CuInSe_2$ chalcopyrite semiconductor. *Phys. Rev. B*, 57:9642–9656, 1998.

[25] C. Domain, S. Laribi, S. Taunier, and J. F. Guillemoles. *Ab initio* calculation of intrinsic point defects in $CuInSe_2$. *J. Phys. Chem. Sol.*, 64(9-10):1657–1663, 2003.

[26] Y. J. Zhao, C. Persson, S. Lany, and A. Zunger. Why can $CuInSe_2$ be readily equilibrium-doped n-type but the wider-gap $CuGaSe_2$ cannot? *Appl. Phys. Lett.*, 85:5860–5862, 2004.

[27] C. Persson, Y. J. Zhao, S. Lany, and A. Zunger. n-type doping of $CuInSe_2$ and $CuGaSe_2$. *Phys. Rev. B*, 72:035211, 2005.

[28] S. Lany and A. Zunger. Anion vacancies as a source of persistent photoconductivity in II-VI and chalcopyrite semiconductors. *Phys. Rev. B*, 72:035215, 2005.

[29] T. Maeda and T. Wada. First-principles calculation of defect formation energy in chalcopyrite-type $CuInSe_2$, $CuGaSe_2$ and $CuAlSe_2$. *J. Phys. Chem. Sol.*, 66:1924–1927, 2005.

[30] S. Lany and A. Zunger. Light- and bias-induced metastabilities in $Cu(In,Ga)Se_2$ based solar cells caused by the (V_{Se}-V_{Cu}) vacancy complex. *J. Appl. Phys.*, 100:113725, 2006.

[31] T. Maeda, T. Takeichi, and T. Wada. Systematic studies on electronic structures of $CuInSe_2$ and the other chalcopyrite related compounds by first principles calculations. *Phys. Stat. Sol. A*, 203:2634–2638, 2004.

[32] S. Lany and A. Zunger. Intrinsic DX centers in ternary chalcopyrite semiconductors. *Phys. Rev. Lett.*, 100:016401, 2008.

[33] W. N. Shafarman and S. Siebentritt and L. Stolt. $Cu(InGa)Se_2$ Solar Cells. In *Handbook of Photovoltaic Science and Engineering*. John Wiley & Sons, 2011.

[34] A. Janotti and C. G. Van De Walle. Native point defects in ZnO. *Phys. Rev. B*, 76(16), 2007.

[35] P. Ágoston, K. Albe, R. M. Nieminen, and M. J. Puska. Intrinsic n-type behavior in transparent conducting oxides: a comparative hybrid-functional study of In_2O_3, SnO_2, and ZnO. *Phys. Rev. Lett.*, 103:245501, 2009.

[36] S. Lany and A. Zunger. Comment on Intrinsic n-type behavior in transparent conducting oxides. *Phys. Rev. Lett.*, 106:069601, 2011.

[37] P. Ágoston, K. Albe, R. M. Nieminen, and M. J. Puska. Reply: Intrinsic n-type behavior in transparent conducting oxides: a comparative hybrid-functional study of In_2O_3, SnO_2, and ZnO. *Phys. Rev. Lett.*, 106:069602, 2011.

[38] J. Heyd, G. E. Scuseria, and M. Ernzerhof. Hybrid functionals based on a screened Coulomb potential. *J. Chem. Phys.*, 118:8207, 2003.

[39] J. Paier, R. Asahi, A. Nagoya, and G. Kresse. Cu_2ZnSnS_4 as a potential photovoltaic material: a hybrid Hartree-Fock density functional theory study. *Phys. Rev. B*, 79:115126, 2009.

[40] J. Vidal, S. Botti, P. Olsson, J.-F. Guillemoles, and L. Reining. Strong interplay between structure and electronic properties in $CuIn(S,Se)_2$: a first-principles study. *Phys. Rev. Lett.*, 104:056401, 2010.

[41] J. E. Jaffe and A. Zunger. Anion displacements and the band-gap anomaly in ternary ABC_2 chalcopyrite semiconductors. *Phys. Rev. B*, 27(8):5176–5179, 1983.

[42] J. E. Jaffe and A. Zunger. Electronic structure of the ternary chalcopyrite semiconductors $CuAlS_2$, $CuGaS_2$, $CuInS_2$, $CuAlSe_2$, $CuGaSe_2$, and $CuInSe_2$. *Phys. Rev. B*, 28:5822–5847, 1983.

[43] S. B. Zhang, S.-H. Wei, and A. Zunger. Stabilization of ternary compounds via ordered arrays of defect pairs. *Phys. Rev. Lett.*, 78:4059–4062, 1997.

[44] G. Makov and M. C. Payne. Periodic boundary conditions in *ab initio* calculations. *Phys. Rev. B*, 51:4014–4022, 1995.

[45] P. Hohenberg and W. Kohn. Inhomogeneous electron gas. *Phys. Rev.*, 136:B864–871, 1964.

[46] W. Kohn and L. J. Sham. Self-consistent equations including exchange and correlation effects. *Phys. Rev.*, 140:A1133–1138, 1965.

[47] W. Kohn. Nobel lecture: electronic structure of matter – wave functions and density functionals. *Rev. Mod. Phys.*, 71:1253, 1999.

[48] S. Kümmel and L. Kronik. Orbital-dependent density functionals: Theory and applications. *Rev. Mod. Phys.*, 80:3–60, 2008.

[49] P. Mori-Sánchez, A. J. Cohen, and W. Yang. Localization and delocalization errors in density functional theory and implications for band-gap prediction. *Phys. Rev. Lett.*, 100:146401, 2008.

[50] A. D. Becke. A new mixing of Hartree-Fock and local density-functional theories. *J. Chem. Phys.*, 98:1372, 1993.

[51] J. P. Perdew, M. Ernzerhof, and K. Burke. Rationale for mixing exact exchange with density functional approximations. *J. Chem. Phys.*, 105:9982–9985, 1996.

[52] J. P. Perdew, K. Burke, and M. Ernzerhof. Generalized gradient approximation made simple. *Phys. Rev. Lett.*, 77:3865–3868, 1996.

[53] J. Heyd, G. E. Scuseria, and M. Ernzerhof. Erratum: Hybrid functionals based on a screened Coulomb potential. *J. Chem. Phys.*, 124:219906, 2006.

[54] W. Paszkowicz, R. Lewandowska, and R. Bacewisz. Rietveld refinement for $CuInSe_2$ and $CuIn_3Se_5$. *J. Alloy. Compd.*, 362:241–247, 2004.

[55] Ariswan, G. El Haj Moussa, F. Guastavino, and C. Llinares. Band gap of $CuInSe_2$ thin films fabricated by flash evaporation determined from transmission data. *J. Mater. Sci. Lett.*, 21:215–217, 2002.

[56] G. Kresse and J. Furthmüller. Efficient iterative schemes for *ab initio* total-energy calculations using a plane-wave basis set. *Phys. Rev. B*, 54:11169–11186, 1996.

[57] G. Kresse and J. Furthmüller. Efficiency of *ab initio* total energy calculations for metals and semiconductors using a plane-wave basis set. *Comp. Mater. Sci.*, 6:15–50, 1996.

[58] M. C. Payne, M. P. Teter, D. C. Allan, T. A. Arias, and J. D. Joannopoulos. Iterative minimization techniques for *ab initio* total-energy calculations: molecular dynamics and conjugate gradients. *Rev. Mod. Phys.*, 64:1045–1097, 1992.

[59] G. Kresse and J. Joubert. From ultrasoft pseudopotentials to the projector augmented wave method. *Phys. Rev. B*, 59:1758, 1999.

[60] J. Hafner. *Ab-Initio* simulations of materials using VASP: Density-functional theory and beyond. *J. Comput. Chem.*, 29(13):2044–2078, 2008.

[61] C. G. Van de Walle and J. Neugebauer. First-principles calculations for defects and impurities: applications to III-nitrides. *J. Appl. Phys.*, 95:3851–3879, 2004.

[62] H.-P. Komsa, T. T. Rantala, and A. Pasquarello. Finite-size supercell correction schemes for charged defect calculations. *Phys. Rev. B*, 86:045112, 2012.

[63] C. Freysoldt, J. Neugebauer, and C. G. Van de Walle. Fully *ab initio* finite-size corrections for charged-defect supercell calculations. *Phys. Rev. Lett.*, 102:016402, 2009.

[64] C. W. M. Castleton, A. Höglund, and S. Mirbt. Managing the supercell approximation for charged defects in semiconductors: Finite-size scaling, charge correction factors, the band-gap problem, and the *ab initio* dielectric constant. *Phys. Rev. B*, 73:035215, 2006.

[65] C. W. M. Castleton, A. Höglund, and S. Mirbt. Density functional theory calculations of defect energies using supercells. *Model. Simul. Mater. Sci. Eng.*, 17:084003, 2009.

[66] J. Shim, E.-K. Lee, Y. J. Lee, and R. M. Nieminen. Density-functional calculations of defect formation energies using supercell methods: Defects in diamond. *Phys. Rev. B*, 71:035206, 2005.

[67] A. Seidl, A. Görling, P. Vogl, J. A. Majewski, and M. Levy. Generalized Kohn-Sham schemes and the band-gap problem. *Phys. Rev. B*, 53:3764–3774, 1996.

[68] S. Lany. Predicting Polaronic Defect States by Means of Generalized Koopmans Density Functional Calculations. In *Advanced Calculations for Defects in Materials*. Wiley-VCH, 2011.

[69] H.-P. Komsa and A. Pasquarello. Assessing the accuracy of hybrid functionals in the determination of defect levels: Application to the As antisite in GaAs. *Phys. Rev. B*, 84(7), 2011.

[70] R. Ramprasad, H. Zhu, P. Rinke, and M. Scheffler. New perspective on formation energies and energy levels of point defects in nonmetals. *Phys. Rev. Lett.*, 108:066404, 2012.

[71] G. Henkelman and H. Jónsson. Improved tangent estimate in the nudged elastic band method for finding minimum energy paths and saddle points. *J. Chem. Phys.*, 113(22):9978–9985, 2000.

[72] A. Janotti and C. G. Van de Walle. LDA+U and Hybrid Functional Calculations for Defects in ZnO, SnO_2, and TiO_2. In *Advanced Calculations for Defects in Materials*. Wiley-VCH, 2011.

[73] P. Deák, B. Aradi, T. Frauenheim, and A. Gali. Challenges in *ab initio* defect modeling. *Mat. Sci. Eng. B*, 154-155:187–192, 2008.

[74] J. L. Lyons, A. Janotti, and C. G. Van De Walle. Why nitrogen cannot lead to p-type conductivity in ZnO. *Appl. Phys. Lett.*, 95:252105, 2009.

[75] J. Paier, M. Marsman, K. Hummer, G. Kresse, I. C. Gerber, and J. G. Angyan. Screened hybrid density functionals applied to solids. *J. Chem. Phys.*, 125(24), 2006.

[76] A. Janotti and C. G. Van De Walle. Fundamentals of zinc oxide as a semiconductor. *Rep. Prog. Phys.*, 72(12), 2009.

[77] U. Gerstmann. *Ab initio* Green's Function Calculation of Hyperfine Interactions for Shallow Defects in Semiconductors. In *Advanced Calculations for Defects in Materials*. Wiley-VCH, 2011.

[78] G. Zhang, A. Canning, N. Grønbech-Jensen, S. Derenzo, and L.-W. Wang. Shallow impurity level calculations in semiconductors using *Ab Initio* methods. *Phys. Rev. Lett.*, 110:166404, 2013.

[79] K. Becker and S. Wagner. Temperature-dependent nuclear magnetic resonance in $CuInX_2$ (X=S,Se,Te) chalcopyrite-structure compounds. *Phys. Rev. B*, 27:5240–5249, 1983.

[80] S. Soltz, G. Dagan, and D. Cahen. Ionic mobility and electronic junction movement in $CuInSe_2$. *Solid State Ionics*, 28-30:1105–1110, 1988.

[81] C. Stephan, S. Schorr, M. Tovar, and H.-W. Schock. Comprehensive insights into point defect and defect cluster formation in $CuInSe_2$. *Appl. Phys. Lett.*, 98(9), 2011.

[82] D. Huang and C. Persson. Stability of the bandgap in Cu-poor $CuInSe_2$. *J. Phys. Condens. Mat.*, 24(45):455503, 2012.

[83] D. Rudmann. *Effects of sodium on growth and properties of Cu(In,Ga)Se_2 thin films and solar cells*. PhD thesis, Swiss Federal Institute of Technology, Zürich, 2004.

[84] M. Kemell, M. Ritala, and M. Leskelä. Thin film deposition methods for $CuInSe_2$ solar cells. *Crit. Rev. Solid State Mat. Sci.*, 30:1–31, 2005.

[85] M. Turcu, O. Pakma, and U. Rau. Interdependence of absorber composition and recombination mechanism in $Cu(In,Ga)(Se,S)_2$ heterojunction solar cells. *Appl. Phys. Lett.*, 80:2598, 2002.

[86] M. Turcu and U. Rau. Fermi level pinning at CdS/$Cu(In,Ga)(Se,S)_2$ interfaces: effect of chalcopyrite alloy composition. *J. Phys. Chem. Sol.*, 64:1591–1595, 2003.

[87] M. Turcu and U. Rau. Compositional trends of defect energies, band alignments, and recombination mechanisms in the $Cu(In,Ga)(Se,S)_2$ alloy system. *Thin Solid Films*, 431-432:158–162, 2003.

Aalto-DD 143/2013

ISBN 978-952-60-5330-1
ISBN 978-952-60-5331-8 (pdf)
ISSN-L 1799-4934
ISSN 1799-4934
ISSN 1799-4942 (pdf)

Aalto University
School of Science
Department of Applied Physics
www.aalto.fi

BUSINESS + ECONOMY

ART + DESIGN + ARCHITECTURE

SCIENCE + TECHNOLOGY

CROSSOVER

DOCTORAL DISSERTATIONS